AD A

Estimating Chemical and Bulk Properties of Middle Distillate Fuels from Near-Infrared Spectra

INTERIM REPORT
TFLRF No. 348

by

S.A. Hutzler
S.R. Westbrook
U.S. Army TARDEC Fuels and Lubricants Research Facility (SwRI)
Southwest Research Institute
San Antonio, TX

Under Contract to

U.S. Army TARDEC
Petroleum and Water Business Area
Warren, MI 48397-5000

Contract No. DAAK70-92-C-0059

July 2000

Disclaimers

The findings in this report are not to be construed as an official Department of the Army position unless so designated by other authorized documents.

Trade names cited in this report do not constitute an official endorsement or approval of the use of such commercial hardware or software.

DTIC Availability Notice

Qualified requestors may obtain copies of this report from the Defense Technical Information Center, Attn: DTIC-OCC, 8725 John J. Kingman Road, Suite 0944, Fort Belvoir, Virginia 22060-6218.

Disposition Instructions

Destroy this report when no longer needed. Do not return it to the originator.

Estimating Chemical and Bulk Properties of Middle Distillate Fuels from Near-Infrared Spectra

INTERIM REPORT
TFLRF No. 348

by

S.A. Hutzler
S.R. Westbrook
U.S. Army TARDEC Fuels and Lubricants Research Facility (SwRI)
Southwest Research Institute
San Antonio, TX

Under Contract to

U.S. Army TARDEC
Petroleum and Water Business Area
Warren, MI 48397-5000

Contract No. DAAK70-92-C-0059

Approved for public release; distribution unlimited

July 2000

Approved by:

Edwin C. Owens, Director
U.S. Army TARDEC Fuels and Lubricants
Research Facility (SwRI)

REPORT DOCUMENTATION PAGE

Form Approved
OMB No. 0704-0188

1. AGENCY USE	2. REPORT DATE	3. REPORT TYPE AND DATES COVERED
	July 2000	Interim, October 1993 - May 1999

4. TITLE AND SUBTITLE
Estimating Chemical and Bulk Properties of Middle Distillate Fuels from Near-Infrared Spectra

5. FUNDING NUMBERS
WD 21
phase 211

DAAK70-92-C-0059

6. AUTHOR(S)
Hutzler, S.A., and Westbrook, S.R.

7. PERFORMING ORGANIZATION NAME(S) AND ADDRESS(ES)
U.S. Army TARDEC Fuels and Lubricants Research Facility (SwRI)
Southwest Research Institute
P.O. Drawer 28510
San Antonio, Texas 78228-0510

8. PERFORMING ORGANIZATION REPORT NUMBER

IR TFLRF No. 348

9. SPONSORING/MONITORING AGENCY NAME(S) AND ADDRESS(ES)
U.S. Army TACOM
U.S. Army TARDEC Petroleum and Water Business Area
Warren, MI 48397-5000

10. SPONSORING/ MONITORING AGENCY REPORT NUMBER

11. SUPPLEMENTARY NOTES

12a. DISTRIBUTION/AVAILABILITY
approved for public release; distribution unlimited

12b. DISTRIBUTION CODE

13. ABSTRACT (Maximum 200 words)
Recent military operations have identified an immediate need for a rapid means of identifying and analyzing fuels in the field. Fuel types requiring analysis are primarily those for ground vehicles and support equipment, including diesel, gasoline and kerosene. The use of improper or contaminated fuels can be detrimental to equipment, resulting in more frequent maintenance problems, shortened lifetimes of fuel-related components (e.g. fuel filter), and in some cases complete failure. As a result, an increase in combat service support on or near the battlefield is required as maintenance personnel and spare parts must be readily available. Common contaminants in fuels include water, biological growth, and by-products of normal fuel degradation. In addition, the quality of host nation fuel resources and captured fuels may be inferior. Other than visual inspection, the only means available for analyzing fuels of questionable quality in the field requires transportation to a non-combat site, mobile laboratory, or other facility with analytical equipment. Therefore, the military is interested in acquiring simple, rugged instrumentation appropriate for field use and capable of rapidly determining fuel type and quality.

Although a number of analytical techniques are available for fuel analysis, only a handful are useful in determining a fuel's suitability for consumption. Some of these include density, viscosity, aromatic content, net heat of combustion, cetane number, boiling point, and the cold temperature properties (e.g. cloud point, pour point, freeze point). Futhermore, some of these properties (e.g. density and net heat of combustion) may be used to discriminate fuel type. Chemometrics is a branch of chemistry that uses mathematical and statistical routines to model a variety of chemical and physical properties. Focusing primarily on middle distillate fuels (diesel fuel and kerosene), this report discusses the use of near-infrared spectroscopy and chemometrics for estimating several pertinent fuel properties. Methods of fuel type discrimination and ways to compensate for instrumental drift through instrument standardization will also be disucssed.

14. SUBJECT TERMS
Chemometrics Near-IR Infrared Spectroscopy Fuel Analysis

15. NUMBER OF PAGES
48

16. PRICE CODE

17. SECURITY CLASSIFICATION OF REPORT	18. SECURITY CLASSIFICATION OF THIS PAGE	19. SECURITY CLASSIFICATION OF ABSTRACT	20. LIMITATION OF ABSTRACT

EXECUTIVE SUMMARY

Problems and Objectives: Military operations in Grenada, Panama, and more recently the Gulf War have identified an immediate need for a rapid means of identifying and analyzing fuels in the field. Fuels requiring analysis include diesel, kerosene, and gasoline used primarily in ground vehicles and support equipment. Common fuel contaminants include water, biological growth, and by-products of normal fuel degradation. Contaminated fuels can be detrimental to vehicles and equipment, resulting in more frequent maintenance problems, shortened lifetimes of fuel related components (e.g., fuel filters), and complete equipment failure. Therefore, maintenance personnel and spare parts must be kept available on the battlefield. Many fuel problems reportedly stem from host nation fuel resources and captured fuels.

The primary goal of this project was to show that near-infrared spectroscopy can be used to determine fuel type and quality with sufficient accuracy to be useful in the field. This work focused on diesel fuel because it is the primary fuel for ground combat and support vehicles.

Importance of Project: Currently, fuel quality in the field is determined using the *Clear and Bright Test* (ASTM D4860). Soldiers collect a fuel sample, hold it up to the light, and look for heterogeneous material (e.g., particulates, dirt, rust, biological growth), emulsified water, or multiple phases. Suspended or emulsified water gives the fuel a hazy appearance thus it fails the brightness test. While this test is satisfactory for identifying gross contamination of the fuel, it cannot identify chemical contamination, contamination due to fuel degradation, or other subtle changes that may affect vehicle performance. It is also not capable of identifying fuel type. The Clear and Bright Test is also poorly suited for large scale distribution such as a bulk fuel farm where thousands of gallons may be dispensed daily. The need for frequent sampling makes it an ineffective method for preventing vehicle contamination. Alternatively, a fuel sample can be collected and transported to a mobile laboratory or other facility. While providing a complete characterization of the fuel sample, the analysis may often span several days and is impractical for situations where timing is critical. Therefore, the U.S. Army and U.S. Marine Corps are interested in acquiring instrumentation that can rapidly identify and evaluate the condition of a fuel.

Technical Approach: To be suitable for military purposes, the instrumentation must meet several minimum requirements. The equipment must 1) be ruggedized for field use, 2) be capable of withstanding harsh environments (i.e. cold/hot, wet/dry climates), 3) give accurate real-time results, 4) require a minimal amount of consumables (e.g., solvents), and 5) be simple to operate. Although it is not a requirement, an emerging trend in the military is to incorporate more commercial products that save time and money in research, development, and acquiring replacement parts. Therefore, commercial off-the-shelf (COTS) technology was used for both hardware and software where possible.

Accomplishments: At the present time, the following properties are being considered for use in the field: density, total aromatics, kinematic viscosity, net heat of combustion, and cetane index. These properties provide the most useful information about a fuel and its suitability for consumption. Additional properties are available, such as cloud point and 50% boiling point, provided that the degree of accuracy is acceptable. For use in the field, limits can be set to determine a pass/fail decision for a given fuel. These limits can be based on an actual fuel specification or specifications that are believed to be appropriate.

Overall, the work was accomplished successfully. Future work should focus on reducing the size of the related hardware, including other fuel types (e.g., gasoline) and investigating other fuel properties.

FOREWORD/ACKNOWLEDGMENTS

This work was performed by the U.S. Army TARDEC Fuels and Lubricants Research Facility (TFLRF) located at Southwest Research Institute (SwRI), San Antonio, Texas, during the period October 1993 through May 1999 under Contract No. DAAK70-92-C-0059. The work was funded and administered by the U.S. Army Tank-Automotive RD&E Center, Petroleum and Water Business Area, Warren, Michigan. Mr. Luis Villahermosa (AMSTA TR-D/210) served as the TARDEC contracting officer's representative and project technical monitor.

The authors would like to acknowledge the efforts of the following: Dr. George E. Fodor, Marilyn S. Voigt, and Leo L. Stavinoha.

TABLE OF CONTENTS

LIST OF TABLES

LIST OF ILLUSTRATIONS

SYMBOLS AND ABBREVIATIONS

1-ArH	Monocyclic Aromatics, mass%
2-ArH	Dicyclic Aromatics, mass%
3-ArH	Tricyclic Aromatics, mass%
AOTF	Acousto-Optic Tunable Filter
API	American Petroleum Institute
ASTM	American Society for Testing and Materials
BP10	Boiling point @10% recover, °C
BP50	Boiling point @50% recover, °C
BP90	Boiling point @90% recover, °C
BP95	Boiling point @95% recover, °C
BPEP	End Boiling Point, °C
C/H	Carbon-to-Hydrogen ratio (C/H)
Carbon	Carbon content, mass%
CCI4737	Cetane Index (ASTM D4737)
CCI976	Cetane Index (ASTM D976)
Cloud	Cloud Point, °C
cm^{-1}	Wavenumbers
Density	Density at 15°C, g/ml
DS	Direct Standardization
ev	Validation Bias
Flash	Flash Point, °C
Freeze	Freeze Point, °C
Hydrogen	Hydrogen content, mass%
IBP	Initial Boiling Point, °C
MD	Mahalanobis Distance
MTBE	*tert*-Butyl methyl ether
NEMA	National Electrical Manufacturers Association
NHC (MJ/Kg)	Net Heat of Combustion, MJ/Kg
nm	Nanometers
PCA	Principal Component Analysis
PC	Principal Component
PDS	Piecewise Direct Standardization
PLS	Partial Least Squares
Pour	Pour Point, °C
ppm	parts per million
RF	Radio Frequency
SDV	Standard Deviation of Validation Errors
SECV	Standard Error of Prediction for Cross-Validation
SEP	Standard Error of Prediction
SwRI	Southwest Research Institute
t	t-test
Total ArH	Total Aromatics, mass%
Viscosity	Kinematic Viscosity at 40°C, cSt

1.0 INTRODUCTION

Military operations in Grenada, Panama, and more recently the Gulf War have identified an immediate need for a rapid means of identifying and analyzing fuels in the field. Fuels requiring analysis include diesel, kerosene, and gasoline used primarily in ground vehicles and support equipment. Common fuel contaminants include water, biological growth, and by-products of normal fuel degradation. Contaminated fuels can be detrimental to vehicles and equipment, resulting in more frequent maintenance problems, shortened lifetimes of fuel related components (e.g., fuel filters), and complete equipment failure. Therefore, maintenance personnel and spare parts must be kept available on the battlefield. Many fuel problems reportedly stem from host nation fuel resources and captured fuels.

Currently, fuel quality in the field is determined using the *Clear and Bright Test* (ASTM D4860). Soldiers collect a fuel sample, hold it up to the light, and look for heterogeneous material (e.g., particulates, dirt, rust, biological growth), emulsified water, or multiple phases. Suspended or emulsified water gives the fuel a hazy appearance thus it fails the brightness test. While this test is satisfactory for identifying gross contamination of the fuel, it cannot identify chemical contamination, contamination due to fuel degradation, or other subtle changes that may affect vehicle performance. It is also not capable of identifying fuel type. The Clear and Bright Test is also poorly suited for large scale distribution such as a bulk fuel farm where thousands of gallons may be dispensed daily. The need for frequent sampling makes it an ineffective method for preventing vehicle contamination. Alternatively, a fuel sample can be collected and transported to a mobile laboratory or other facility. While providing a complete characterization of the fuel sample, the analysis may often span several days and is impractical for situations where timing is critical. Therefore, the U.S. Army is interested in acquiring instrumentation that can rapidly identify and evaluate the condition of a fuel.

To be suitable for military purposes, the instrumentation must meet several minimum requirements. The equipment must 1) be ruggedized for field use, 2) be capable of withstanding harsh environments (i.e., cold/hot, wet/dry climates), 3) give accurate real-time results, 4) require a minimal amount of consumables (e.g., solvents), and 5) be simple to operate. Although it is not a requirement, an emerging

trend in the military is to incorporate more commercial products that save time and money in research, development, and acquiring replacement parts. Therefore, commercial off-the-shelf (COTS) technology was used for both hardware and software where possible.

Near-infrared spectroscopy was identified as an analytical technique capable of accomplishing this task. Near-infrared spectrometers based on acousto-optic tunable filter (AOTF) technology have no moving parts and employ high energy sources and low noise detectors. This results in a rugged instrument with a high signal-to-noise ratio. The instruments are routinely housed in stainless steel enclosures with internal climate controls for use in factories and plants. Therefore, the instruments could easily be adapted for military use.

The primary goal of this project was to show that near-infrared spectroscopy can be used to determine fuel type and quality with sufficient accuracy to be useful in the field. This work focused on diesel fuel because it is the primary fuel for ground combat and support vehicles.

2.0 BACKGROUND AND THEORY

2.1 Near-Infrared Spectroscopy

The most utilized portion of the near-infrared region is between 1000 and 2500 nm (10,000 - 4,000 cm^{-1}). For organic molecules, near-infrared spectra are the result of combination and overtone bands of the fundamental vibrational frequencies seen in the mid-infrared region. [1] Overtone bands appear at integer multiples (approximately) of the fundamental vibrational frequencies, and each subsequent overtone is dramatically weaker in intensity. The first overtone for a fundamental vibrational frequency in the mid-infrared region appears at twice the wavenumber (or one half of the wavelength), the second overtone appears at three times the wavenumber (or one third of the wavelength), etc. For this reason, near-infrared spectra are typically comprised of first and second overtones of C-H, N-H, and O-H vibrational modes. This makes near-infrared spectroscopy highly suitable for use with hydrocarbon fuels. However, to be useful, a correlation must exist between the minor spectral differences related to fuel composition and the fuel property of interest.

A typical near-infrared spectrum for diesel fuel is shown in Figure 1. The relatively smooth features that result from overlapping and colinear spectral responses make the spectra nearly useless for qualitative spectral interpretation. However, with the increasing power of desktop computers and emerging mathematical treatments, the correlation of chemical and physical properties to small spectral differences can now be elucidated. The result is a system that can rapidly identify a fuel and estimate a variety of its properties related to its suitability for consumption by a vehicle.

By looking at model compounds, some approximate peak assignments can be made. Figures 2, 3, and 4 show the spectra for isooctane (2,2,4-trimethylpentane), methyl *t*-butyl ether (MTBE) and

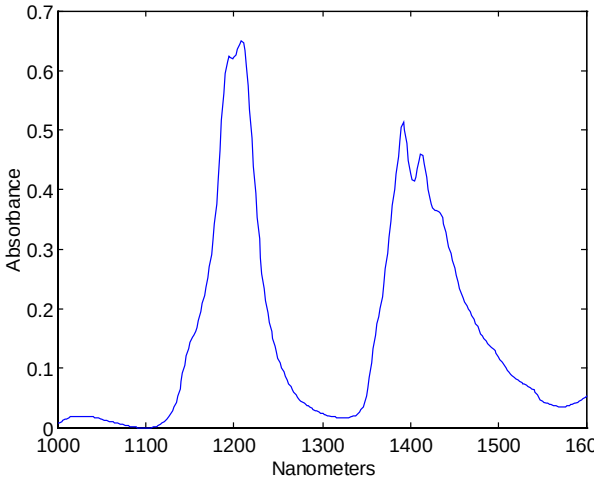

Figure 1. Diesel Fuel Near-Infrared Spectrum

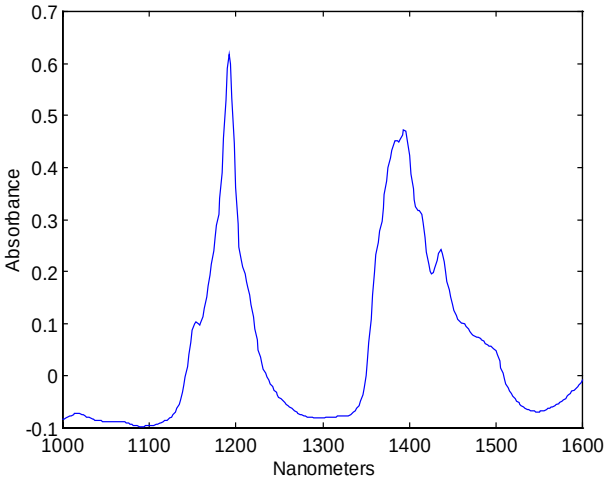

Figure 2. Near-Infrared Spectrum of Isooctane

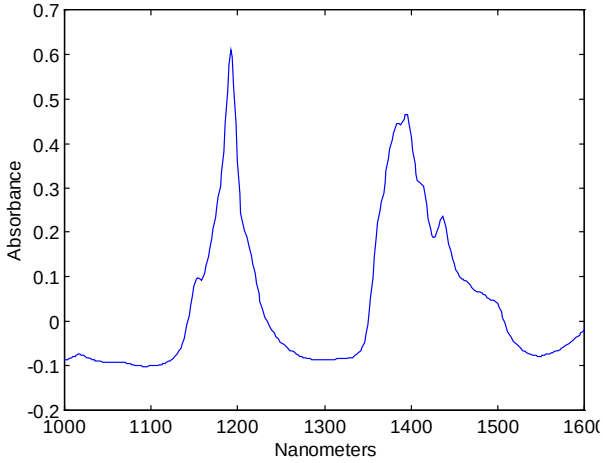

Figure 3. Near-Infrared Spectrum of MTBE

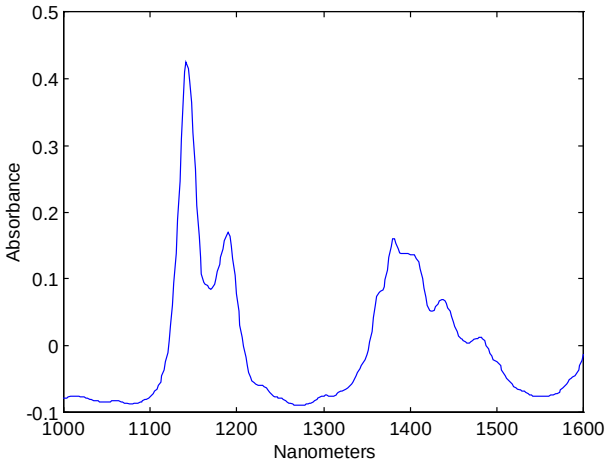

Figure 4. Fuel Near-Infrared Spectrum of Toluene

toluene, respectively. There are strong similarities between the spectra of isooctane and MTBE. The two compounds share similar features in that both have only sp^3 hybridized carbon and each contains a *t*-butyl group. The dominant near-infrared absorptions from each molecule should be attributable primarily to sp^3 C-H bonds. Isooctane has sp^3 C-H bonds in the form of methyl (CH_3), methylene (CH_2), and methine (CH) groups while MTBE has only methyl groups. Since sp^3-sp^3 C-C bonds show only weak absorptions in mid-band spectra, they are not expected to contribute substantially to the near-infrared spectra. The C-O bond from MTBE may also contribute to the spectra as an overtone but to a lesser extent. The C-O stretch is more likely to contribute to the spectra in conjunction with other fundamental vibrations as a combination band. In fact, any absorption at approximately 1500 cm^{-1} or less would have to appear as a 4th overtone or higher and consequently would be very weak in intensity.

In addition to the sp^3 C-H bonds, toluene also contains sp^2 C-H bonds, sp^2-sp^2 C-C bonds, and an sp^2-sp^3 C-C bond. As a result, there are some significant differences between the spectra of isooctane (Figure 2) and toluene (Figure 4); these differences can be used to make some approximate peak assignments. The predominant absorptions for toluene should be attributable to the sp^3 and sp^2 C-H bonds. The small peak that appears at approximately 1150 nm in isooctane becomes the dominant absorption in toluene. This wavelength appears to be largely correlated to the aromatic character because of its coincidental increase in intensity as the aromatic character of the sample increased; however, the peak is not entirely due to the aromatic character since there is also a small absorption at that wavelength in isooctane. The second overtone for an sp^2 C-H stretching vibration (3008 cm^{-1}≈3324 nm) should appear at approximately 1108 nm (3324 nm/3). For isooctane, the peaks at 1200 nm and 1350-1500 nm show much stronger absorptions than the peak at 1150 nm and thus appear to be strongly correlated to the aliphatic character (sp^3 C-H) of the molecule. The reverse is true for toluene (i.e., the peak at 1150 nm has a stronger absorption than those at 1200 nm and 1350-1500 nm). The second overtone for an sp^3 C-H ($\nu_s CH_3$) stretching vibration (2872 cm^{-1} ≈ 3482 nm) should appear at approximately 1161 nm (3482 nm/3). In each calculation, there is a discrepancy of 40 nm in wavelength position, which is not unexpected considering the broad bands in the near-infrared spectra and the approximate nature of the

calculation; the calculation is an approximation of an anharmonic oscillator model where the anharmonicity value, if taken into account, may be has high as 5%. [1] The apparent reversal in absorption between the bands at 1150 nm and at 1200 nm and 1350-1500 nm correlates well with the relative ratios of aliphatic and aromatic character in each molecule.

2.2 AOTF

The main component of an AOTF spectrometer is the AOTF crystal. [2] For the near-infrared region, this crystal is most commonly made of Tellurium Oxide (TeO_2). A transducer mounted to one side of the crystal vibrates when radio frequency (RF) is applied to it and acoustic waves are emitted into the crystal. The acoustic waves create refractive index variations in the crystal, which then act as a transmission diffraction grating. The crystal behaves more like a filter because it only allows one specific wavelength of light to be diffracted through the beam slit at a given applied RF. Therefore, any wavelength in the range of the instrument can be randomly accessed by applying the appropriate RF, hence the name 'tunable filter'.

2.3 Chemometrics

First coined by Dr. Bruce Kowalski (University of Washington) in 1975, chemometrics is a branch of chemistry that applies mathematical and statistical routines to chemical and physical data. The goal is to relate the state (i.e., a chemical or physical characteristic) of a system to measurements (e.g., spectral data) collected on the system. In many cases, rather than measuring individual chemical components, a bulk property of the system (like density) is sought. The term given to this type of observation is *indirect* [3,4] because the value of the bulk property is inferred from the overall chemical composition of the system. This is entirely feasible because the chemical composition governs the value of the bulk property and is reflected in the spectral data. All that remains is to uncover the mathematical relationship between the spectral data and that property. This work focuses on generating linear calibration models which assume that the bulk property and the spectra result from linear combinations of the individual chemical components found in fuel. This does not imply that alternative calibration methods (e.g., non-linear

regression or neural networks) are not suitable. Instead, it was believed that the linear methods would give sufficiently accurate property estimations and could be easily adapted for use in the field (i.e., be easily reprogrammed into a single integrated software package for instrument control and fuel-property estimation).

A significant factor contributing to the popularity and growth of chemometrics is that the vast amounts of spectral data being generated by today's analytical instruments is not being utilized to its potential. Chemometric routines compress the spectra by extracting only the essential information and leaving behind most of the noise and redundancies. The result is that the changes in the spectra can be described using far fewer variables without a significant loss of relevant information. Nevertheless, the compressed spectral data is only useful if it can be correlated to the property data (e.g., fuel properties). Two commonly used and widely accepted routines for this type of data analysis, Principal Component Analysis (PCA) and Partial Least Squares (PLS) Regression, are discussed briefly below.

2.4 Fuel Properties and Analysis

Most standard petroleum test methods are established by the American Society for Testing and Materials (ASTM), the American Petroleum Institute (API), the Institute of Petroleum (IP), and the military. These routine test methods are widely accepted and are commonplace in typical petroleum analytical laboratories. Nevertheless, these test methods have a number of significant disadvantages. Many require expensive equipment, hazardous chemicals and solvents, large volumes of sample, sample preparation, and extended testing periods. Near-infrared spectroscopy combined with chemometrics can eliminate or reduce most of these requirements provided the selected fuel property can be correlated to the spectra.

Table 1 contains a list of the analyses [5] that were utilized in this study and the abbreviations by which they will be referred to throughout this text. *Density* is not a significant measure of fuel quality, but it can be used as an indicator of aromatic content and fuel type. *Cloud*, *Pour*, and *Freeze Points* describe the low-temperature characteristics of the fuel. *Cloud Point* is the temperature at which the paraffinic constituents of a fuel may be precipitated as a wax, while the *Pour Point* is the lowest temperature at which a fuel can be pumped. The *Freeze Point* is the lowest temperature at which a fuel can be used

Table 1
Fuel Properties and Abbreviations

Property	ASTM Test Method	Abbreviation
Density at 15 C, g/mL	D 4052	Density
Freeze Point, °C	D 2386	Freeze Point
Flash Point, °C	D 93	Flash Point
Cloud Point, °C	D 2500	Cloud Point
Pour Point, °C	D 97	Pour Point
Kinematic Viscosity at 40°C, cSt	D 445	Viscosity
Initial Boiling Point, °C	D 86	IBP
Boiling Point @ 10% recovery, °C	D 86	BP10
Boiling Point @ 50% recovery, °C	D 86	BP50
Boiling Point @ 90% recovery, °C	D 86	BP90
Boiling Point @ 95% recovery, °C	D 86	BP95
End Boiling Point, °C	D 86	BPEP
Cetane Index (2 variable method)	D 976	CCI976
Cetane Index (4 variable method)	D 4737	CCI4737
Hydrogen Content, mass%	D 5291	Hydrogen
Carbon Content, mass%	D 5291	Carbon
Carbon-to-Hydrogen ratio (C/H)	D 5291	C/H
Net Heat of Combustion, MJ/Kg	D 240	NHC
Monocyclic Aromatics, mass%	D 5186	Mono-ArH
Dicyclic Aromatics, mass%	D 5186	Di-ArH
Tricyclic Aromatics, mass%	D 5186	Tri-ArH
Total Aromatics, mass%	D 5186	Total-ArH

without the risk of hydrocarbons solidifying. The *Flash Point* of a fuel is the temperature to which the fuel must be heated to produce an ignitable vapor-air mixture above the liquid fuel when exposed to an ignition source. The *Viscosity* of a fuel is a measure of its resistance to flow and can affect its combustion properties and its ability to be pumped. Distillation (*Boiling Point*) characteristics of a fuel strongly influence its performance. Expressed in terms of percent recovered, the boiling point of a fuel reflects its volatility. High volatility can result in vapor lock, while low volatility leads to reduced fuel economy through poor fuel atomization. *Cetane Number* is a numerical result of an engine test designed to measure a diesel (or distillate) fuel's ignition quality.[5] Preliminary studies [6] showed cetane number to

give poor correlations with near-infrared spectra; the poor correlations were most likely due to the poor reproducibility of the engine test. As an alternative, *Cetane Index*, a calculated cetane number, was used. Two methods of calculating cetane index were investigated in this study. The two-variable method (ASTM D 976) uses density (ASTM D 1298) and 50% boiling point (ASTM D 86), while the four-variable method uses density (ASTM D 1298) and 10%, 50%, and 90% boiling points (ASTM D 86) to calculate cetane index. *Carbon* and *Hydrogen Content* and *Carbon/Hydrogen Ratio* are not used significantly for evaluating fuel quality; however, they can be used to ascertain the oxidation state of a fuel. *Net Heat of Combustion (MJ/Kg)* is a measure of the heat produced by a fuel upon complete burning and is thus related to fuel economy. *Monocyclic*-, *Dicyclic*-, and *Tricyclic-aromatics* are defined as the mass percent of one, two, and three-ring aromatics, respectively, found in a fuel. The *Total Aromatic Content* is the mass percent of all aromatics found in the fuel.

Based on previous work, [6,7] some fuel properties were excluded from this work because of their poor correlations to near-infrared spectra: Steam Jet Gum (ASTM D 381), Total Water (ASTM D 1744), Total Sulfur (ASTM D 4294), Wear Scar Diameter (High Frequency Reciprocating Rig, ISO/CD 12156 and Ball-On-Cylinder Lubricity Evaluator, ASTM D 5001), and Fuel Lubricity (U.S. Army Scuffing Load Wear Test). Additional properties were omitted because they could be calculated from properties already present or were determined using other simple and more accurate methods. Net Heat of Combustion, BTU/lb (ASTM D 240), was removed in favor of the smaller numerical values given by Net Heat of Combustion, MJ/kg (ASTM D 240). API Gravity (D 1298 and D 4052) and Density (D 1298) were omitted, since they can be calculated from one another. Density determined by ASTM D 4052 (an instrumental method) was preferred to the manual method of ASTM D 1298.

Table 2 contains the repeatability and reproducibility data for the ASTM methods used in this study. This precision data is reported in each ASTM method and is determined by statistical examination of interlaboratory cross-checks. Repeatability is defined as the difference between two single and independent results obtained by the same operator from the same apparatus under the same operating conditions using identical test materials. Reproducibility is defined as the difference between two single and independent results obtained by different operators working in different laboratories on identical

Table 2
Repeatability and Reproducibility of the Standard ASTM Procedures

Property	ASTM Test	Repeatability	Reproducibility
Density at 15 C, g/mL	D 4052	0.0001	0.0005
Freeze Point, °C	D 2386	1.0	2.5
Flash Point, °C	D 93	2.0	3.5
Cloud Point, °C	D 2500	2.0	4.0
Pour Point, °C	D 97	3.0	6.0
Kinematic Viscosity at 40 C, cSt	D 445	0.14 @ 3	0.44 @ 3
Initial Boiling Point, °C	D 86	3.5	8.5
Boiling Point @ 10% recovery, °C	D 86	4.5	9.5
Boiling Point @ 50% recovery, °C	D 86	4.5	9.5
Boiling Point @ 90% recovery, °C	D 86	5.0	12.0
Boiling Point @ 95% recovery, °C	D 86	5.0	12.0
End Boiling Point, °C	D 86	3.5	10.5
Cetane Index (2 variable method)	D 976	calculated	3.3[a]
Cetane Index (4 variable method)	D 4737	calculated	3.3[a]
Hydrogen Content, mass%	D 5291	0.42 @ 13%	0.83 @ 13%
Carbon Content, mass%	D 5291	0.98 @ 87%	2.44 @ 87%
Carbon-to-Hydrogen ratio (C/H)	D 5291	calculated	calculated
Net Heat of Combustion, MJ/Kg	D 240	0.13	0.40
Monocyclic Aromatics, mass%	D 5186	0.7	4.0
Dicyclic Aromatics, mass%	D 5186	0.7	4.0
Tricyclic Aromatics, mass%	D 5186	0.7	4.0
Total Aromatics, mass%	D 5186	0.7	4.0

material. In general, one sample in 20 may exceed the reported values for repeatability and reproducibility under those conditions. For this work, the reproducibility data was used as the criteria for acceptance of a given calibration model. These numbers represent values that are achievable in the real world (i.e., they are based on results from more than one laboratory and operator).

2.5 Fuel Characteristics

Although fuels are varied and complex mixtures, they are composed primarily of varying ratios of aromatics and aliphatics that differ in their substitution patterns and degree of branching. These

differences affect the behavior of the fuel and ultimately determine the fuel type. For example, compared to a diesel fuel, a kerosene typically has a higher net heat of combustion and lower total aromatics, density, freeze point, and viscosity. Several correlations between bulk fuel properties and chemical composition can be derived from the oxidation state of the fuel, which is proportional to the ratio of unsaturated (i.e., aromatics and olefins) to saturated (i.e., aliphatics) components. The higher concentration species will impart more of their characteristics on the fuel, which affect the fuel's behavior. The total aromatic content is inversely proportional to cetane number, net heat of combustion, and cloud point and is directly proportional to the carbon-to-hydrogen ratio, density, and viscosity. As the aromatic content increases, the carbon-to-hydrogen ratio increases resulting in a decrease in the net heat of combustion. The poorer combustion characteristics lead to a reduced cetane number. Alternatively, higher concentrations of aliphatics will raise the cold temperature properties and decrease the density.

3.0 METHODOLOGY

3.1 Calibration Procedure

Figure 5 shows a step-by-step procedure of the general calibration process for building Partial Least Squares (PLS) models.[8] Initially, a set of fuel samples is collected that is representative of the types of fuels to be analyzed. This set should be diverse and contain as many variations as might be expected in future samples. For PLS, a small number of samples (2-50) may be used, but generally the more samples used, the more robust the calibration. This is especially true for fuels where the samples may have an essentially infinite number of possible variations because of the large number of constituents in each sample. Hundreds of samples are commonly employed for developing fuel calibrations. For each fuel sample, an infrared spectrum is collected, and the desired laboratory analyses (ASTM or other reference method) are run. Once the data is collected, the sample set is typically split into two unique sets: a calibration training set and a validation set. The calibration set contains the samples with which the calibration will be built. This set should cover the widest range of fuel property values. Once the models are built, the samples in the validation set are used to test the model.

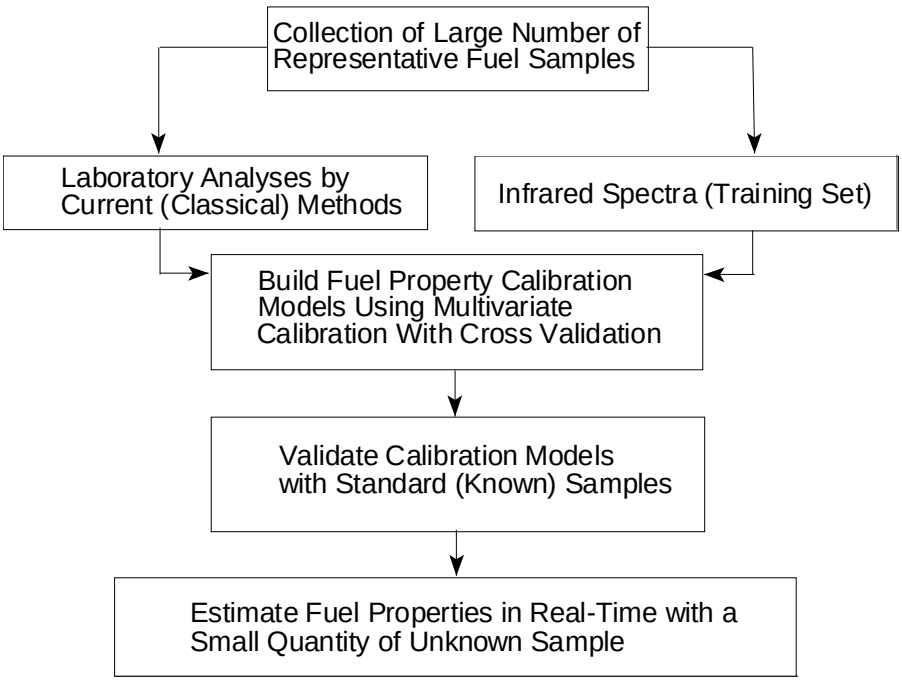

Figure 5. General Calibration Procedure

Multivariate modeling is subjective by nature because of the numerous variables and decisions that require user input. There are no strict guidelines for building calibrations, and most calibrations are developed through trial and error. The process of model building is also a dynamic one in that the models can be periodically updated. New or unique samples may appear that are not present in the model. If these samples are found to be acceptable after analysis by the classical laboratory procedures, then the samples could be added to the calibration set and the model rebuilt. The model would then be able to recognize this type of sample if it were encountered again. To reiterate, the goal is to build the model using samples that are representative of the types of samples that are expected to be analyzed.

The most important aspect of the calibration process is the *cross-validation.* Cross-validation is a computationally intensive procedure used to generate statistics on the model being built. During cross-validation, a given number of samples are removed from the calibration set. Using the remainder of the samples in the set, a calibration model is built and used to estimate the property value of those samples that were removed. Samples may be left out one at a time, in blocks, or in any interval. For this work, every 10th sample was removed from the calibration set during each cross-validation rotation; the square root of the number of samples up to ten is a general guideline used to determine the number of times to

split the data set during a cross-validation. Therefore, in each rotation, approximately 40 samples were removed from the calibration set and their properties estimated with models built from the rest of the samples. The cross-validation procedure is repeated until each sample has been left out at least once. Since the samples that are removed are true unknowns to the calibration model (i.e., the sample is not included in the calibration model), the predictive power of the model is revealed. The information obtained from a cross-validation can be used to select the proper number of factors for the model and to identify possible outliers, both of which are discussed below.

3.2 Preprocessing [9,10]

Three data pre-treatments were utilized in an attempt to optimize the calibration models.

3.2.1. Mean-centered spectra were generated by subtracting the mean spectrum from each spectrum of the calibration training set. The mean spectrum is generated by averaging each wavelength for all of the spectra in the calibration training set. In general, mean-centering enhances the minor spectral differences related to fuel composition by removing a major component of useless spectral variation, the non-zero mean.

3.2.2. First-difference spectra were generated by calculating the arithmetic difference between the individual points of the raw spectral data. For a spectrum, $\mathbf{x}$, with n points, the first-difference spectrum would be: $[(\mathbf{x}_2-\mathbf{x}_1), (\mathbf{x}_3-\mathbf{x}_2), ...(\mathbf{x}_n-\mathbf{x}_{n-1})]$. The resultant first-difference spectrum would contain n-1 points. Using first-difference preprocessing corrects any baseline offsets in the spectra. Mid-infrared spectra typically do not suffer from substantial baseline offsets, unlike near-infrared spectra where baseline offsets are commonplace and some form of baseline correction is usually essential.

3.2.3. Second-difference spectra are generated by taking the first difference of a first-difference spectrum. The result is a spectrum with n-2 points. Using second-difference preprocessing corrects the baseline offset and any sloping of the baseline.

Any noise in the original spectra will be amplified in difference spectra. Fortunately, the advantage inherent to AOTF spectrometers is their relatively low noise. Indeed, it was discovered that our analyses

were not hampered by noise in the original or difference spectra. For this reason, first and second differences were chosen over true derivatives. Difference spectra also have the added advantage of being simpler to calculate.

3.3 Principal Component Analysis (PCA) and Partial Least Squares (PLS) Regression

The factor-based methods, PCA and PLS, create a simplified version of the spectroscopic data by a process known as spectral decomposition.[8] Although spectra may contain many different variations in absorbance and baseline, many of the variations are unrelated to the sample or are redundant (e.g., detector and environmental noise, differences in sampling handling, interactions between different chemical species). The goal is to extract a set of "variation spectra" (called *loadings* or *principal components (PC)* in PCA and *factors* or *latent variables* in PLS) that only represent the differences between the spectra at each wavelength. These spectra are used to generate the calibration models rather than the raw spectra. The variation spectra would be fewer in number than the original spectra but would contain the same number of wavelengths. As a result, model computation time would be reduced. Ideally, by applying a scaling constant to each loading and linearly summing over all of the loadings, the original spectra can be closely reconstructed. The scaling constants are referred to as *scores*. The scores are said to describe the relationship between the samples, while the loadings describe the relationship between the wavelengths. The PCA decomposition is illustrated below.

For PCA, the matrix expression for the model equation is shown in Equation 1. $\mathbf{X}$ is an $m \times n$ matrix of spectral absorbances, $\mathbf{t}$ is an $m \times 1$ score vector, $\mathbf{p}$ is an $n \times 1$ loading vector, $\mathbf{T}$ is an $m \times f$ matrix of score values, $\mathbf{P}$ is an $f \times n$ matrix of loadings, and $\mathbf{E}$ is an $m \times n$ residual matrix, where m is the number of samples, n is the number of wavelengths, and k is the number of PCs.

$$\boldsymbol{X} = \boldsymbol{t}_1\boldsymbol{p}_1^{T} + \boldsymbol{t}_2\boldsymbol{p}_2^{T} + \bullet\bullet\bullet + \boldsymbol{t}_k\boldsymbol{p}_k^{T} + \boldsymbol{E} = \boldsymbol{T}_k\boldsymbol{P}_k^{T} + \boldsymbol{E} \qquad \text{Equation 1}$$

The **tp** pairs are ordered by the amount of variance that they capture so each successive **tp** pair captures less variance and more noise.

Both PCA and PLS use this spectral decomposition technique but for different purposes. PCA is not a regression technique; rather, it is used to calculate the loadings and scores for inspection of the data. PCA is strictly based on the spectra and does not use the property data in any way. PLS on the other hand is a powerful modeling technique that utilizes both the spectra and the property data in the decomposition process. As a result, a correlation is constructed between the changes in the spectra and the changes in the property data, which can be applied to unknown spectra to estimate the property of interest. In addition to the spectral decomposition shown in Equation 1, PLS simultaneously decomposes the property value matrix in an analogous manner. The two sets of scores that are generated are presumably related to each other, and a linear regression is performed to model that relationship. Although PLS is more difficult to illustrate and understand, the important thing to remember is that PLS attempts to find those factors that are correlated to the property data while also describing large amounts of the variance in the wavelength data. Several excellent manuscripts describing PCA/PLS are available in the literature.[11-14]

3.4 Outlier Statistics

The PLS routines output several plots for aiding in outlier detection during the calibration process. Predicted *vs.* Actual (shown later) and Leverage *vs.* Studentized Residuals [9] (example shown in Figure 6) help identify *possible* outliers. In a Leverage *vs.* Studentized Residual plot, a large residual (>3) indicates that a sample could have an incorrect property value; a high leverage indicates that a sample has a large influence on the model, perhaps because it is unique in some way, the property data is incorrect, or the spectrum was run incorrectly. Two other plots that are useful for outlier detection are that of Q *vs.* Sample Number and T^2 *vs.* Sample Number [9] (examples shown in Figures 7 and 8, respectively). Q measures the amount of variation a sample has *outside* of the factors defined for the model. Stated otherwise, it measures the amount of non-deterministic variation left over after the

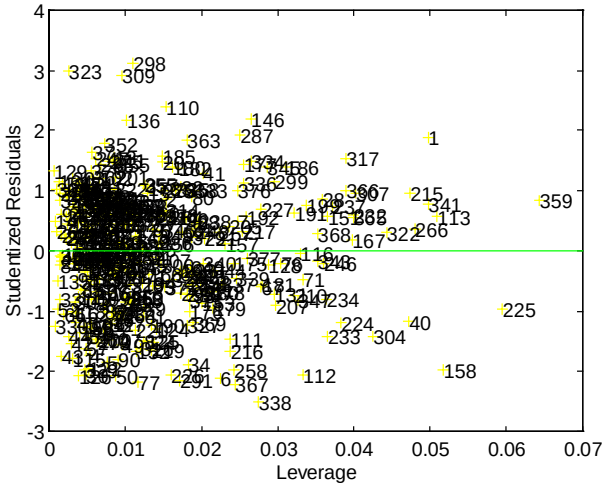

Figure 6. Leverage vs. Studentized Residuals

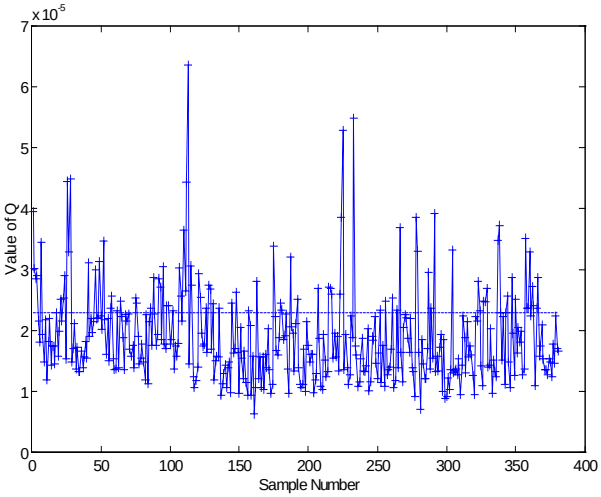

Figure 7. Q vs. Sample Number

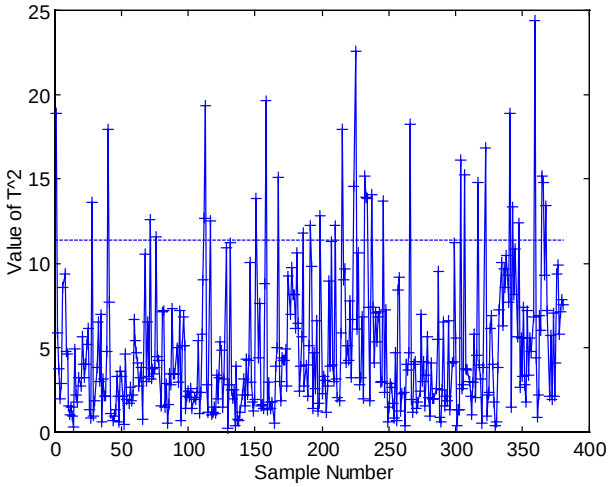

Figure 8. T^2 vs. Sample Number

deterministic variation has been removed. T^2 measures the distance of the sample from the multivariate mean (i.e., within the model). The plots clearly indicate those samples that have unusual values of Q and T^2 thereby identifying them as possible outliers. Ultimately, the user must decide if the sample should be removed from the set given the information that is available and what is known about the samples.

Another measure, known as Mahalanobis Distance (MD),[15,16,17] denoted D^2, was used to verify that the calibration model was appropriate for the sample. The MD is calculated in terms of standard deviation (i.e., the numerical result is equivalent to a standard deviation). Those calibration samples that were used to construct the final calibration model for density were used in Equation 2 (**X** is the spectral matrix) to generate the Mahalanobis matrix, **M**.

$$M=(X^TX)^{-1} \qquad \text{Equation 2}$$

A different Mahalanobis matrix must be generated for each fuel type. To calculate D^2 for an unknown sample, Equation 3 was applied where vector **a** is the unknown spectrum and **M** is the Mahalanobis matrix generated from Equation 2.

$$D^2=aMa^T \qquad \text{Equation 3}$$

Once calculated, D^2 can be utilized in several ways.[16,17] One use considers those samples with $D^2>3$ (standard deviations) to be outliers. In practice, this was found to be too lenient; too many samples were

being considered acceptable while their estimated numbers were unacceptable. An alternate application considers a sample an outlier only if it exceeded a preset maximum, D^2_{max}. To determine D^2_{max} each sample was removed from the calibration set and its D^2 value calculated based on the remaining samples. The D^2_{max} was the sample with the highest D^2. While this method appears to be too strict it was found to give the most reliable results. Ultimately, Mahalanobis Distance will only be used to warn the user of a possible outlier. Critical decisions concerning the use of the fuel must still be made by a human operator.

3.5 Calibration and Validation Statistics

The following are definitions that will be used throughout the remainder of the text. They are similar in that they attempt to measure the average error in a given model. [9]

3.5.1. <u>Standard Error of Prediction for Cross-Validation, SECV.</u> *SECV* is the measure of a model's ability to predict property values of new samples that are <u>not</u> a part of the calibration model. The samples being predicted are those that are removed during each rotation of a cross-validation. In Equation 4, y_i' is the predicted value of sample *i* for a given property, y_i is the known value of that property (i.e., the reference value) for that sample, and *n* is the number of samples in the calibration set.

$$SECV = SEP = \sqrt{\frac{\sum_{i=1}^{n}(y_i' - y_i)^2}{n}} \qquad \text{Equation 4}$$

3.5.2. <u>Standard Error of Prediction, *SEP*</u>. After a final calibration model has been constructed, the model is again validated using a separate set of validation samples that were not part of the original calibration set and therefore not included in the model. Equation 4 still applies with the same variable definitions as above.

In each calculation, the value that is calculated has the same units as the original fuel property and represents the standard deviation in the differences between the predicted and estimated values. The *SEP* and *SECV* are typically used for comparing similar calibration models built with different parameters.

3.6 Assessing the Validity of the Model

In fact, there are no guidelines by which calibration models can be judged other than the criteria required for a particular user and application. The ASTM methods are primary methods for determining a particular fuel property and no other methods exist for verifying their accuracy. Instead, ASTM commonly conducts round-robin tests to generate precision statements based on the results from many laboratories, and this is assumed to be the allowable 'error' in the method. In ASTM E 1655-97, *Standard Practices for Infrared Multivariate Quantitative Analysis*,[17] (at the time of this writing, the current test method is ASTME 1655-99) several methods are offered for determining the validity of a regression model. These methods aid in selecting those calibration models that provide the best results.

The *Validation Bias*, e_v, is given in Equation 5 where y_i is the reference value, y_i' is the predicted value, and n is the number of samples.

$$e_v = \sqrt{\frac{\sum_{i=1}^{n}(y_i - y_i')}{n}} \qquad \text{Equation 5}$$

The validation bias gives the average bias for the estimation of the validation set and can show whether the estimated values are strongly skewed in a positive or negative direction. The presence of a strong bias may indicate a source of systematic error in the measurements. Ideally, an average bias near zero is preferred since it indicates only random errors in the measurements.

Using e_v, the *Standard Deviation of Validation Errors*, *SDV*, is calculated using Equation 6.

$$SDV = \sqrt{\frac{\sum_{i=1}^{n}\left[(y_i - y_i') - e_v\right]^2}{n-1}} \qquad \text{Equation 6}$$

Once e_v and *SDV* are calculated, Equation 7 can be applied to determine if the validation bias is significant.

$$t = \frac{e_v\sqrt{n}}{SDV} \qquad \text{Equation 7}$$

Equation 7 performs a *t*-test to determine if the validation estimates show a statistically significant bias. The *t* value can be compared to tabulated critical *t* values for the given number of samples. If the

calculated *t* value is greater than the critical *t* value, then there is a 95% probability that the model will not give the same average result as the reference method. Thus, the model's validity is considered suspect.

To determine if the estimated values from the model agree with the values determined by the reference method, ASTM E 1655-97 offers a simple approach. Using the reproducibility, *R*, of the ASTM reference method, Equation 8 can be applied, where y_i' is the predicted value and y_i is the reference value.

$$y_i' - R < y_i < y_i' + R \qquad \text{Equation 8}$$

Based on the definition of reproducibility, if 95% of the reference values for the validation set fall within this interval for a given property, then the estimates from the model agree with the reference method as well as a second laboratory repeating the reference measurement would agree.

3.7 Discriminant Analysis

An important aspect of this work was the ability to discriminate between different types of fuels (e.g., diesel fuel *vs.* gasoline). A number of routines exist for this purpose and most commercial chemometric packages incorporate one or more. The work presented here focuses on a simple Euclidean distance measure (Equation 9). Like samples will tend to form clusters that are distinguishable from other dissimilar samples. The Euclidean based method attempts to assign a sample to a particular cluster based on its proximity.

$$distance = \sqrt{(x_1 - x_2)^2 + (y_1 - y_2)^2} \qquad \text{Equation 9}$$

For spectra, at least two wavelengths are chosen where the spectral differences are the greatest between the fuels. Using all available spectra, the mean absorbance is then calculated for each wavelength for each material (e.g., diesel fuel). Using those wavelengths, the distance from an unknown sample to the mean of each material can be calculated using Equation 9 (x_1 and y_1 represent absorbances at the chosen wavelengths for the unknown sample and x_2 and y_2 represent the wavelength means for a given material). The sample is then assigned to the closest cluster. An application of this technique for discriminating diesel fuel and gasoline will be shown below.

3.8 Calibration Transfer

A significant limitation to the use of chemometrics is the difficulty associated with maintaining the stability of an instrument over an extended period of time. Besides the normal spectral variations attributable to the chemical composition of a sample, spectra also contain unintended instrumental and temporal variations.[18] Instrumental responses will vary from one instrument to another and within the same instrument over a period of time. The implication is that calibration models generated for an instrument will need to be updated or corrected many times throughout the life of the instrument. The most obvious way to counter the changing instrumental response is to simply recollect the calibration training set spectra periodically and rebuild the calibration models. However, in practice this is not always a practical solution because the integrity of some samples cannot be sustained indefinitely, the samples may be hazardous, or the process of collecting several hundred spectra may be too time consuming and expensive.

The process known as *calibration transfer* or *instrument standardization* [19,20,21] is a multivariate method used to modify spectra to make them more closely match the response of the instrument at the time the calibration spectra were recorded. In this work, two methods of calibration transfer were investigated: *Direct Standardization* (DS) and *Piece-Wise Direct Standardization* (PDS). Both methods require new standard spectra to be collected for a small subset of the original calibration training spectra. The new standard spectra ($\mathbf{X}_{S,\,new}$) are matched with the old calibration spectra ($\mathbf{X}_{S,\,old}$) and a transformation function, **F**, is determined by a least-squares regression of the data (Equation 10).

$$F=(X_{S,new}^{T}X_{S,new})^{-1}X_{S,new}^{T}X_{S,old} \qquad \text{Equation 10}$$

The **F**-matrix is a square matrix with dimensions of wavelength×wavelength and describes the relation between the new spectra and the old spectra. Used in Equation 11 (where **E** is a residual error matrix), **F** transforms the spectra currently being collected ($\mathbf{X}_{new}$) to appear as though they were run at the same time as the calibration samples. The transformed spectra, $\mathbf{X}_{trans}$, can now be used with the original calibration models.

$$X_{trans}=X_{new}F+E \qquad \text{Equation 11}$$

The main difference between DS and PDS is that DS uses the entire spectrum all at once to generate the transformation function, while PDS uses a small moving window of data points to map the newspectra onto the old.[9] The use of a small window enhances the transformation because each transformed wavelength will be more similar to a small wavelength region on either side of it than to the entire spectrum. Each transformation is based on a small subset of spectra (usually three to nine) that must be selected. For PDS, the window size must also be selected. Since no general guidelines are available for selecting the window size, trial-and-error is often the approach used. Each method can also incorporate a calculation for an additive background correction[22] to improve the accuracy of the transformation. PDS and DS only provide a multiplicative correction for the transformation. In some cases, additional additive corrections are necessary. An example of an additive difference is the source drifting slightly between the background and sample scans. This situation is not expected to arise in this application since backgrounds were collected between each sample. PDS is currently the "gold standard" by which all other calibration transfer methods are judged. The application of each method is discussed below.

4.0 MATERIALS AND DATA PREPARATION

4.1 Instrumentation

Spectra were collected on two near-infrared Luminar [2] spectrometers purchased from Brimrose Corporation of America. The spectrometer designations were as follows: Instrument 1, Luminar 2060, Chemical Process Analyzer, NEMA 12 enclosure, 3-channel multiplexer with two additional cooling units; Instrument 2, Luminar 2000, standard industrial 19-inch rack mount, NEMA 4 enclosure. Both Instruments were equipped with fiber-optic transflectance immersion probes (16-inch length, 1/4-inch diameter) having effective pathlengths of 1 cm and stainless steal conduit for sheathing. The probes and fiber-optic cables were purchased from Custom Sensors and Technologies (CST). Each spectrometer had a wavelength range of 1000-1600 nm (10,000-6,250 cm^{-1}), and spectra were collected in absorbance units as an average of 32 scans at 2-nm resolution. With these parameters, total scan time was less than five seconds. The Luminar spectrometers were designed to run over a network or attached directly to a PC in a laboratory configuration. Experiments were performed in both modes and worked equally well.

Spectra were collected by first running a background in air with the same parameters as above. Without any sample preparation, the clean and dry immersion probe was lowered into the sample container and swirled so that no bubbles were trapped in the window. After the scan, the probe was thoroughly cleaned with HPLC grade *n*-hexanes and blown dry with a stream of dry air or dry nitrogen. As a routine measure, a new background was collected between each sample to ensure that the probe was clean.

4.2 Calculations

Computations were carried out on a 166 MHz Pentium® running Microsoft Windows® NT® 4.0 and a 90 MHz Pentium® running Windows® 95. The multivariate routines used in this work are those supplied in version 1.5.2 of the PLS_Toolbox (Eigenvector Technologies, Manson, WA) module running under MATLAB version 4.2c.1 (Mathworks, Inc., Natick, MA). All spectra were converted from the binary Brimrose format to an ASCII text file containing a single vector of absorbance data. For each instrument and property, the calibration and validation spectra were loaded into MATLAB along with the corresponding fuel property data in matching order.

4.3 Fuel Samples

A large set of fuels was collected at commercial filling stations and military installations worldwide. The samples were collected during three different climatic periods (winter, spring, and summer) to account for any seasonal differences; previous studies [6,7] determined that separate calibration models are not needed for each climatic period because the varying compositional differences are masked by widespread delivery. Fuel types included commercial low sulfur grade diesel fuels and military diesel fuels and kerosenes (e.g., JP-5, JP-8). Each sample was subjected to a battery of 33 chemical and physical analyses. The total number of samples used in this study was 790, approximately 50 of which were identified as kerosenes. When not being analyzed, the samples were stored in the dark at 4°C. Table 3 contains summary property statistics for all of the samples in the data set.

4.4 Calibration and Validation Sets

For the calibration training sets to have the widest possible range and maintain an even distribution of property values, each fuel property in the data matrix was individually sorted in ascending order. Every

Table 3
Summary Statistics for all Samples

Property	Minimum	Maximum	Average
Density	0.7818	0.8728	0.8446
Freeze	-59.5	6.6	-14.0
Flash	23	96	62
Cloud	-60.5	2.1	-17.6
Pour	-75	-3	-30
Viscosity	1.12	4.05	2.52
IBP	99	229	176
BP10	158	256	214
BP50	182	297	258
BP90	204	347	311
BP95	207	375	325
BPEP	217	388	339
CCI976	37.0	59.8	46.8
CCI4737	36.4	65.7	46.9
H	12.29	14.48	13.10
C	82.75	87.73	86.57
C/H	5.921	7.097	6.612
NHC(MJ/Kg)	41.01	43.46	42.69
Mono ArH	7.7	38.9	23.9
Di ArH	0.5	12.8	5.9
Tri ArH	0.0	3.4	1.0
Total ArH	8.3	47.2	30.8

other sample was then selected and assigned to the calibration training set for that fuel property. The remaining samples were assigned to the validation set for the property. The last samples in the calibration and validation sets were swapped to maximize the fuel property value range of the calibration training set. The initial calibration and validation training sets were each composed of 395 fuels. Tables 4 and 5 contain summary property statistics for the calibration and validation training sets, respectively. Note how the statistics for the training sets are similar to those in Table 3, indicating a representative sampling of the full data set for each training set.

Table 4
Summary Statistics for the Calibration Training set, 395 samples

Property	Minimum	Maximum	Average
Density	0.7818	0.8728	0.8446
Freeze	-59.5	6.6	-14.0
Flash	23	96	62
Cloud	-60.5	2.1	-17.6
Pour	-75	-3	-30
Viscosity	1.12	4.05	2.52
IBP	99	229	176
BP10	158	256	214
BP50	182	297	258
BP90	204	347	311
BP95	207	375	325
BPEP	217	388	339
CCl976	37.0	59.8	46.8
CCl4737	36.4	65.7	46.9
H	12.29	14.48	13.10
C	82.75	87.73	86.57
C/H	5.921	7.097	6.611
NHC(MJ/Kg)	41.01	43.46	42.69
Mono ArH	7.7	38.9	23.8
Di ArH	0.5	12.8	5.9
Tri ArH	0.0	3.4	1.0
Total ArH	8.3	47.2	30.7

4.5 Solvent Data

Three solvents were selected as standards for tracking instrument performance. These solvents were selected as they represented different components that may be found in fuels: isooctane (aliphatics), toluene (aromatics), and MTBE (oxygenates). B&J Brand (High Purity Solvent) toluene, isooctane (2,2,4-trimethylpentane), and methyl t-butyl ether (MTBE) were acquired from VWR Scientific Products. For probe cleaning, HPLC grade *n*-hexanes were acquired from Fisher Scientific. Spectra for the three standard solvents were collected on each instrument every day in which fuel samples were run. In this way, an instrument's condition on any given day could be compared to its past performance.

Table 5
Summary Statistics for the Validation Training Set, 395 Sample

Property	Minimum	Maximum	Average
Density	0.7871	0.8726	0.8447
Freeze	-59.4	5.3	-13.9
Flash	33	88	62
Cloud	-60.4	1.3	-17.5
Pour	-75	-6	-30
Viscosity	1.14	3.94	2.52
IBP	132	218	176
BP10	162	256	214
BP50	184	297	258
BP90	210	340	311
BP95	220	361	325
BPEP	240	377	339
CCl976	37.3	59.1	46.8
CCl4737	37.4	64.9	46.9
H	12.36	14.33	13.11
C	83.86	87.61	86.58
C/H	5.951	7.074	6.613
NHC(MJ/Kg)	41.06	43.41	42.69
Mono ArH	8.3	37.8	23.9
Di ArH	0.6	12.0	5.9
Tri ArH	0.0	3.2	1.0
Total ArH	9.3	45.8	30.8

4.6 Reference Fuels

Four reference diesel fuels were acquired from Howell Hydrocarbons & Chemicals, Inc., to aid in the development of calibration models and calibration transfer protocols. The reference fuel designations were as follows: Diesel-1, Howell Cat 1-H (0.4% Sulfur); Diesel-2, Howell Mack Diesel; Diesel-3, Howell 6V92TA; and Howell LSRD4 (**L**ow **S**ulfur **R**eference **D**iesel). A fifth reference, a previously acquired Jet A-1, was also used. The five reference fuels were re-analyzed at SwRI for selected fuel properties (Table 6).

Table 6
Reference Fuel Specifications

Property	Diesel-1	Diesel-2	Diesel-3	Diesel-4	Jet-A1
Density	0.8522	0.8597	0.8523	0.8518	0.7888
Freeze	-4.6	-7.2	-10.4	-14.3	-56.5
Flash	90	65	73	80	54
Cloud	-10.1	-12.1	-14.8	-16.3	-35.4
Pour	-15	-18	-21	-24	-63
Viscosity	3.10	2.17	2.62	2.84	1.14
IBP	220.5	176.2	185.3	199.2	175.9
BP10	243.9	203.1	215.2	220.7	183.0
BP50	271.5	260.2	268.7	264.4	188.3
BP90	319.5	309.1	317.7	318.0	195.7
BP95	334.1	326.4	331.2	328.8	198.0
BPEP	346.0	344.5	340.9	336.5	211.7
CCl976	13.07	12.40	12.96	13.12	14.20
CCl4737	47.9	43.2	47.5	46.6	43.6
H	49.8	41.4	46.6	46.6	45.8
C	86.45	87.38	86.74	86.87	85.65
C/H	6.6144	7.0468	6.6929	6.6212	6.0317
NHC(MJ/Kg)	42.85	42.48	42.77	42.84	43.48
Mono ArH	16.4	32.3	22.3	20.7	13.1
Di ArH	10.0	10.8	8.3	7.6	1.1
Tri ArH	1.1	1.0	1.0	0.6	0.1
Total ArH	27.5	44.1	31.6	28.9	14.2

5.0 EXPLORATORY ANALYSIS USING PCA

5.1 Principal Component Analysis

Prior to constructing models for the fuel properties, a PCA was performed on the set of solvent standards for each instrument. As shown below, the PCA indicated the stability of the instrument over an extended period of time and helped determine the type of preprocessing needed for constructing the calibration models. Since the fuel spectra were collected during the same time frame as the solvents, one can assume that any instrumental anomalies that the solvents were subjected to, so too were the fuel spectra. The discussion will focus on Instrument 1 as an example followed by a summary for Instrument 2.

5.2 PCA Using Mean-Centered Spectra (Instrument 1)

Figures 9-11 show spectra for isooctane, MTBE, and toluene, respectively (each run 27 times). The first and most obvious observation is the baseline offset in all cases. Possible sources for this drift include: source/ detector degradation; changes in external temperature; damage to fiber-optic cables due to improper handling or shifting of probe's reflective surface during use. Further inspection revealed that although the baseline fluctuated from day to day, the overall trend was a positive shift over time. The exact cause of the shifting baseline is unknown.

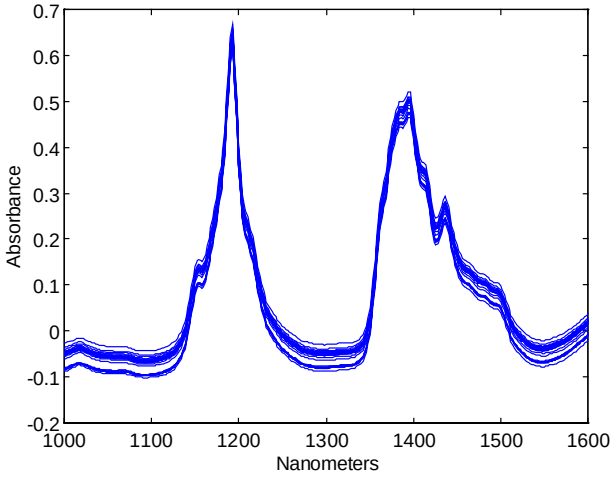

Figure 9. Near-Infrared Spectra of Isooctane, Instr.1.

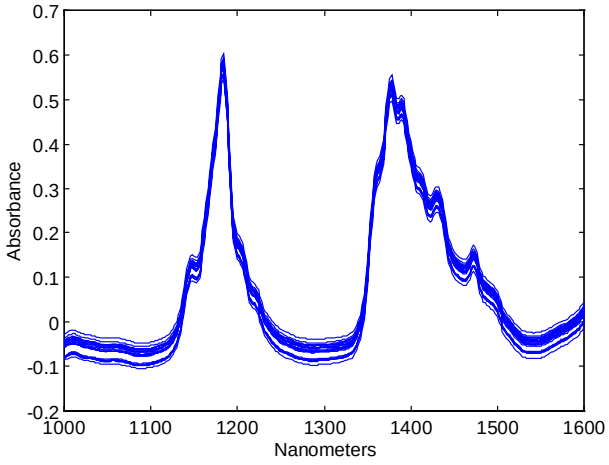

Figure 10. Near-Infrared Spectra of MTBE, Inst. 1.

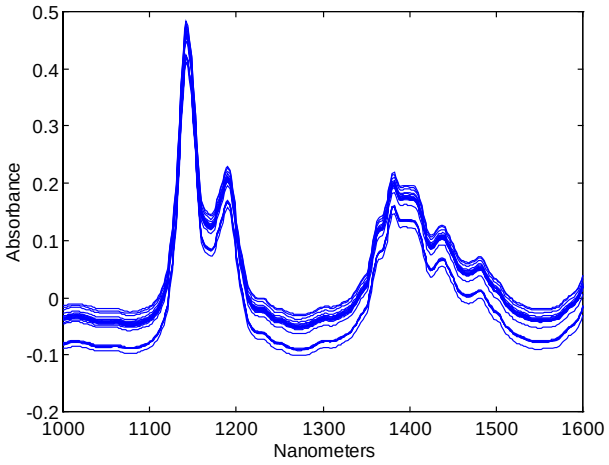

Figure 11. Near-Infrared Spectra of Toluene, Inst. 1.

The combined set of standard solvent spectra (81 total) were mean-centered and a PCA was performed. Table 7 contains the results of the analysis in terms of the percent variance captured by the PCA model. From the table, 3 PCs were deemed sufficient to construct the model. The fourth PC is not added because the percent variance captured by that PC is much less than 1% of the total variation in the spectra. It was arbitrarily assume that the spectra have *at least* 1% variation due to noise and other non-deterministic variation, thus choosing to add this PC would generate an *overfit* model. An overfit model is one that includes noise or other non-relevant information. Plots of the Scores *vs.* Sample number and Loadings *vs.* Variable Number were generated. These plots helped identify the underlying structure in the spectra.

Table 7. Instrument 1: PCA of Solvent Data Using Mean-Centered Spectra

Principal Component Number	Percent Variance Captured	Cumulative Total
1	80.60	80.60
2	13.74	94.34
3	5.65	99.99
4	0.01	100.00

The scores for PC #1 and PC #3, and the loadings for PC #3 are shown in Figures 12-14. Samples 1-27 are isooctane, 28-54 are MTBE, and 55-81 are toluene, with each set ordered as a function of time. In Figure 12, only two "clusters" of data appear where there should be three; the variation in the scores values causes the clusters for isooctane and MTBE to overlap. This variation should not exist since the samples were identical in each cluster. The scores plot for PC #3 (Figure 13) indicates more clearly the severity of the situation. The significant amount of variation within each cluster indicates the instrument's variability during sample collection. The symmetry in the score values among the different solvents also indicates the problem was not random (i.e., a change in the instrument's response at some point in time was reflected in all three solvents). There was a dramatic change in the instrument between the 8th and 9th replication of the solvents, represented by the sharp change in the scores' values. The source of this change is unknown.

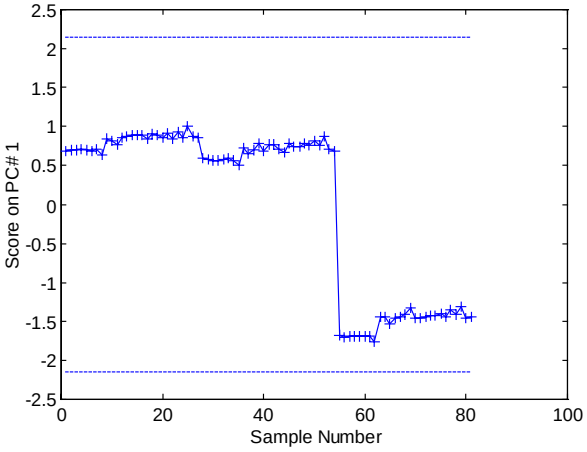

Figure 12. Scores vs. Sample Number for PC#1, Mean-Centered Spectra, Instr. 1

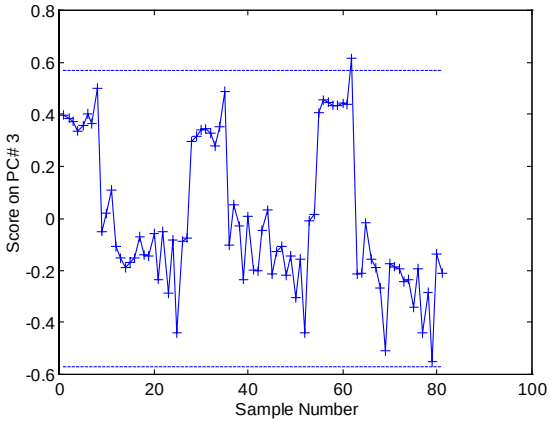

Figure 13. Scores vs. Sample Number for PC#3, Mean-Centered Spectra, Instr. 1

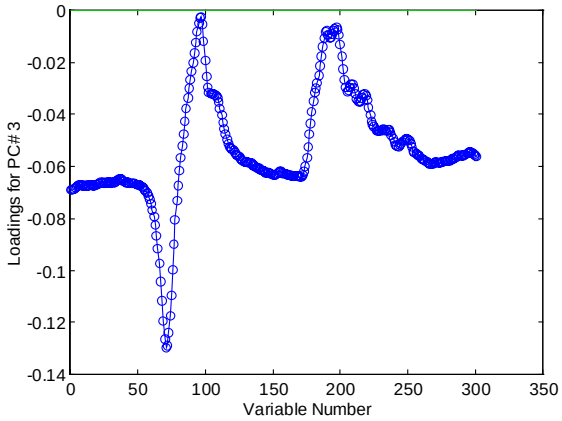

Figure 14. Loading vs. Variable Number for PC#3, Mean-Centered Spectra, Instr. 1

The plot of the Loadings *vs.* Variable number for PC #3 (Figure 14) reveals the possible root of the problem. The loadings show a significant baseline offset from zero, as was seen in Figures 9-11. This implies that the changes in the instrument caused subsequent runs of identical samples to experience baseline shifts. Finally, one last plot is that of the Scores (PC #1) *vs.* Scores (PC #2) seen in Figure 15. Again, this plot shows the clustering for each solvent and the variation within each cluster.

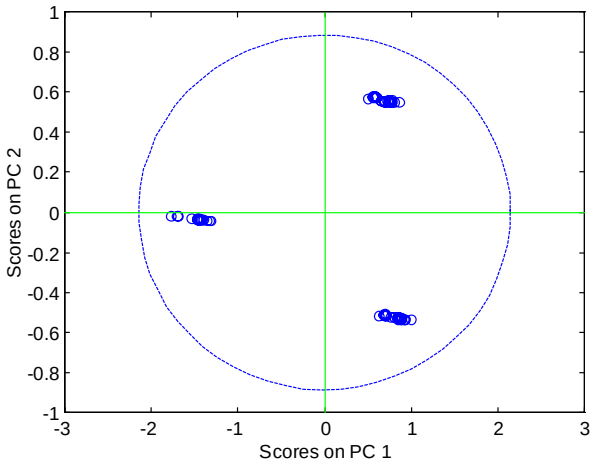

Figure 15. Scores (PC#1) vs. Scores (PC#2), Mean-Centered Spectra, Instr. 1

The poor correlation between like solvents points to the roaming baseline. For a given solvent, the shifting baseline is a large source of variation relative to minor variations due to the chemical composition. Although the exact cause of the baseline shift is unknown, possible explanations include: a decaying source or detector; damage to fiber-optic probes; and temperature fluctuations in the surrounding environment. The goal was to find a method for preprocessing the spectral data that removes this unintended variation. As mentioned earlier, a baseline offset can be removed by calculating a first-difference spectrum. The PCA was repeated, combining first-difference preprocessing and mean-centering to eliminate the baseline offset.

5.3 PCA Using First Difference/Mean-Centered Spectra

Figure 16 shows a first-difference spectrum for isooctane.The previous baseline offset (Figures 9-11) in the other solvent sets is no longer apparent. The data were not smoothed; if the original spectra contained a substantial amount of noise, first-difference preprocessing would amplify that noise, resulting in the need for a smoothing technique. However, in this case no significant change in the noise level is apparent, reconfirming the low noise level in the instrument.

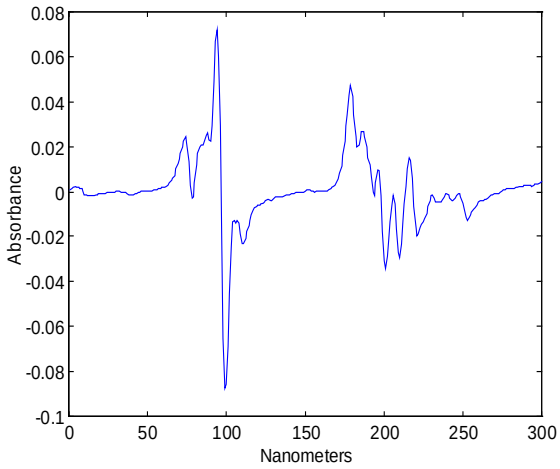

Figure 16. First Difference spectrum for Isooctane, Instr. 1

Table 8
Instrument 1: PCA of Solvent Data Using First Difference/Mean-Centered Spectra.

Principal Component Number	Percent Variance Captured	Cumulative Total
1	57.11	57.11
2	42.85	99.96
3	0.01	99.97
4	0.01	99.98

The results of the PCA are given in Table 8. Notice here that only 2 PCs are required to sufficiently model the three solvents. The reduction in the number of PCs occurs because the model no longer needs to account for the variability in the baseline. Since there are only two major sources of variation in the spectra, *i.e.,* the difference between the aliphatic and aromatic absorptions, only 2 PCs are required to differentiate the three different solvents. In Figure 17, a plot of Scores (PC #1) *vs.* Sample Number, the three distinct clusters are now visible, with less variation within each cluster than seen before in Figure 12. Furthermore, a plot of the Loadings *vs.* Variable Number for PC#2 in Figure 18 shows no evidence of a baseline offset. Finally, a plot of the Scores (PC #1) *vs.* Scores (PC #2) in Figure 19 also indicates less variation within each solvent set.

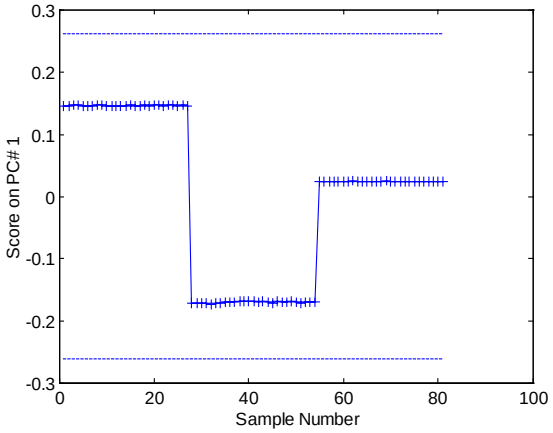

Figure 17. Scores vs. Sample Number for PC#1, First Difference Spectra, Instr. 1

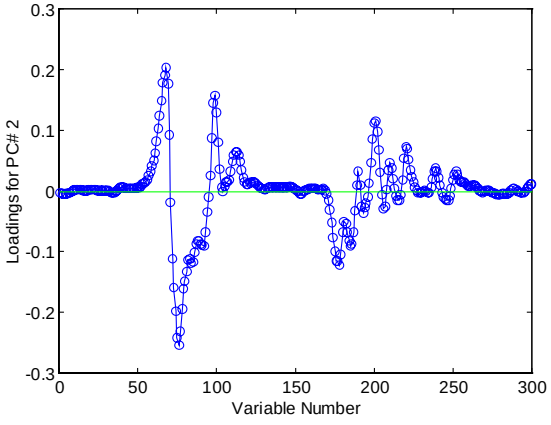

Figure 18. Loading vs. Variable Number for PC#2, First Difference Spectra, Instr. 1

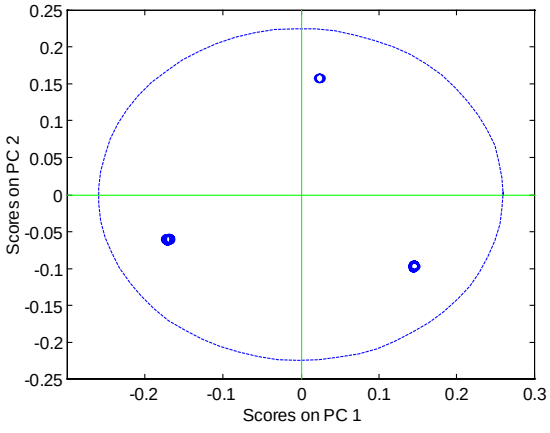

Figure 19. Scores (PC#1) vs. Scores (PC#2), First Difference Spectra, Instr. 1

In conclusion, the PCA of the standard solvents for Instrument 1 indicated that first difference/mean-centered preprocessing would be the best choice for removing the unwanted variation in the spectra as a result of the baseline offset. Due to compositional differences, the fuel spectra will have more variations than the solvent spectra, complicating the situation somewhat; a similar analysis for fuel would be extremely difficult to interpret. Ultimately, the effect that various types of preprocessing have on the fuel spectra can only be determined by construction and comparison of the appropriate calibration models. Nevertheless, as an exploratory tool, PCA of the solvent data (model compounds) helped narrow the preprocessing methods by providing a way to *visualize* the data. Most importantly, the analysis has tentatively ruled out the possibility of a more serious instrument malfunction since the apparent problems in the modeling could be corrected by simply correcting the baseline offset.

A PCA was also run using 2nd difference/mean-centered preprocessing. However, it was abandoned because no additional improvements were seen over first difference/mean-centered preprocessing.

5.4 PCA for Instrument 2

A PCA was run in an identical manner for Instrument 2. The results once again identified first difference/mean-centered preprocessing as necessary to remove the unwanted variations in the baseline. For Instrument 2, Figure 20 shows a plot of the Scores (PC #1) *vs.* Scores (PC #2) based on a 2 PC model of first difference/mean-centered spectra. Based on this information, calibration models were built using first difference/mean-centered spectra and are discussed below.

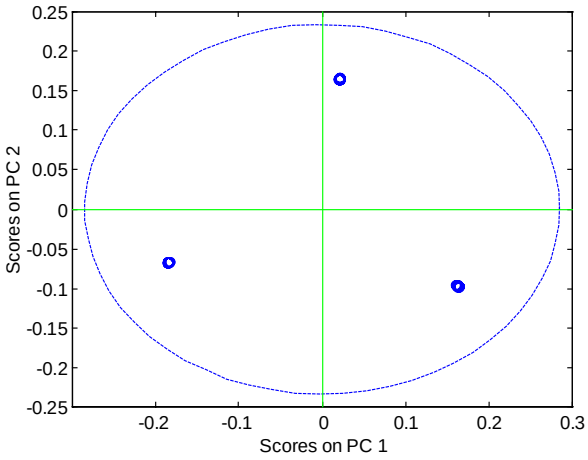

Figure 20. Scores (PC#1) vs. Scores (PC#2), First Difference Spectra, Inst. 2

5.5 Summary

Two suggestions can be made concerning work done in the future. First, the use of the standard solvents should be incorporated into the day-to-day use of the instrument. The solvents provide the capability to

track instrument performance over an extended period using a single component sample that is commonly manufactured to repeatable specifications. Second, collected data should be analyzed daily and compared to previous runs to ensure that the instrument is operating satisfactorily. This way, any malfunction in the instrument can be caught at an early stage and prevent the collection of unusable data.

6.0 FUEL ANALYSIS

6.1 Discriminant Analysis

Figure 21 shows overlaid plots of a diesel fuel and a gasoline. To distinguish these fuels using the simple Euclidian-based discriminant analysis, two wavelengths were selected where large differences in absorption existed between the two fuel types. From first difference spectra, wavelengths 1204 nm and 1386 nm were chosen to discriminate these fuel types. When these wavelengths were plotted against each other for all of the first difference/mean-centered spectra (diesel, kerosene, and gasolines), the result is the plot shown in Figure 22. Because diesel fuel and kerosene are so similar (the clusters severely overlap), they cannot be separated in this manner. However, diesel fuel and kerosene as a single unit were found to be easily distinguishable from gasolines by this method. The two primary clusters that emerge, one for diesel/kerosene and one for gasoline, are well-separated. The mean absorptions were calculated for each wavelength for each cluster and are indicated by the crosshairs. Using these means in Equation 9, unknown samples can be identified as either a diesel/kerosene or a gasoline. Nothing can be gained by adding additional wavelengths to the discrimination. The two-wavelength discrimination was found to be sufficiently accurate to separate middle distillates from gasoline. Since the various middle distillate fuels are indistinguishable by their spectra, adding more wavelengths only complicates the calculation.

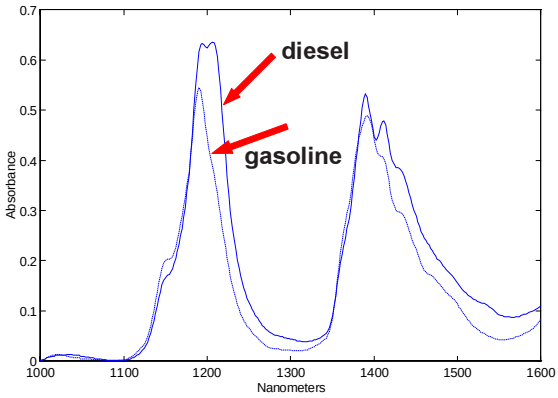

Figure 21. Near-Infrared Spectra of Diesel and Gasoline

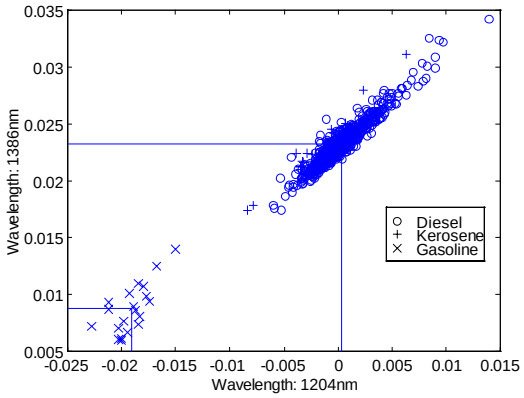

Figure 22. Discriminating Diesel Kerosene, and Gasoline

Currently, to discriminate diesel fuel from kerosene, the estimated value for the net heat of combustion (in MJ/Kg) is being used (diesel fuel if < 43.00 and kerosene if ≥43.00). Other properties, such as density, could also be incorporated for further verification but have not been implemented to date.

As a secondary measure for discrimination, Mahalanobis Distance was used as a method for verifying the fuel type assigned by the Euclidean-based method. To calculate the MD, several channel numbers were selected empirically from first difference/mean-centered spectra. The channels, 12 in total, were selected where major 'absorptions' were seen. As described earlier, the Mahalanobis matrix, **M**, was generated for the diesel fuel and kerosene set. Using D^2_{max} as the criteria for confirmation, the fuel type assignments of the Euclidean-based discrimination may be verified. Although these methods of discrimination have not been rigorously tested to date, preliminary use of these methods proved very encouraging with a very low failure rate. An example of the use of D^2_{max} is shown below in Section 7.0.

6.2 PLS Calibrations

Partial Least Squares calibration models were constructed for Instrument 2 using the first difference/ mean-centered calibration training set spectra. For each model, Table 9 reports the final calibration range, the *SECV*, the *SEP*, and the percent inclusion based on Equation 8 (all calculations were performed after exclusion of outliers using D^2_{max}). Plots of Predicted *vs.* Actual for selected calibration models are shown in Figures 23-28. Additional calibration plots for Predicted *vs.* Actual are located in Appendix A, Figures 1-16.

Plots for the cold temperature properties (cloud point, pour point, and freeze point), flash point, viscosity, and boiling points (BP10, BP50, etc.) each showed a clustering of samples resulting from separation of the diesel fuel and kerosene. Believing that separate models for each fuel type might improve the results, calibration models were constructed for flash point, cloud point, freeze point, pour point, viscosity, and BP50 using only diesel fuels (Table 10 and Figures 29-34, respectively). Separate models for kerosene were not built due to the lack of sufficient samples. As expected, significant improvements (30% reduction in the *SECV*) were seen for the cloud and freeze point calibration models (see Tables 9 and 10).

Table 9
PLS Calibrations for Diesel/Kerosene
Instrument 2, First Difference/Mean-Centered

Property	Calibration Range Min.	Calibration Range Max.	SECV	SEP	% inclusion[a]
Density	0.7883	0.8728	0.0024	0.0024	16.6
Freeze	-59.5	2.3	4.0	5.2	51.8
Flash	38	85	6	7	43.0
Cloud	-60.5	-2.6	4.3	4.5	73.1
Pour	-75	-9	5	18	45.9
Viscosity	1.15	3.92	0.16	0.17	98.2
IBP	139	217	10	11	64.7
BP10	158	256	7	7	87.0
BP50	194	297	5	6	92.6
BP90	223	340	9	12	83.1
BP95	230	358	11	14	74.9
BPEP	249	372	10	12	68.0
CCI976	37.4	59.8	0.8	1.0	99.5
CCI4737	38.3	60.1	0.8	1.1	99.0
H	12.29	14.19	0.08	0.10	100.0
C	84.95	87.73	0.23	0.31	100.0
C/H	5.9213	7.0968	0.0469	0.0513	-
NHC(MJ/Kg)	42.29	43.46	0.06	0.12	100.0
Mono ArH	8.8	38.9	1.1	1.2	99.5
Di ArH	0.5	12.8	0.6	0.6	100.0
Tri ArH	0.0	2.8	0.3	0.3	100.0
Total ArH	10.7	47.2	1.0	1.1	100.0

[a] % inclusion based on Equation 8

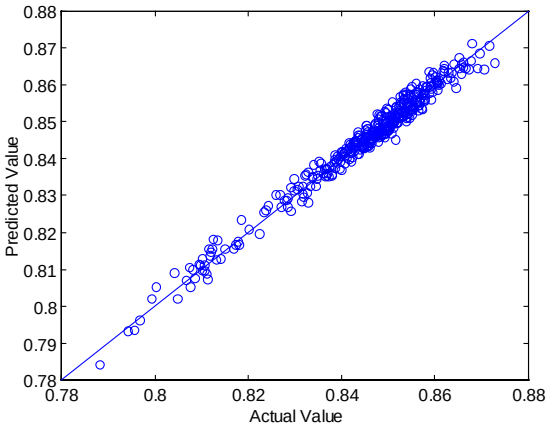

Figure 23. Instr 2: Calibration for Density

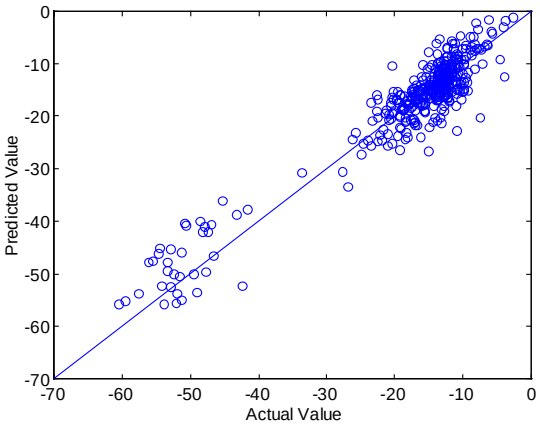

Figure 24. Instr 2: Calibration for Cloud Point

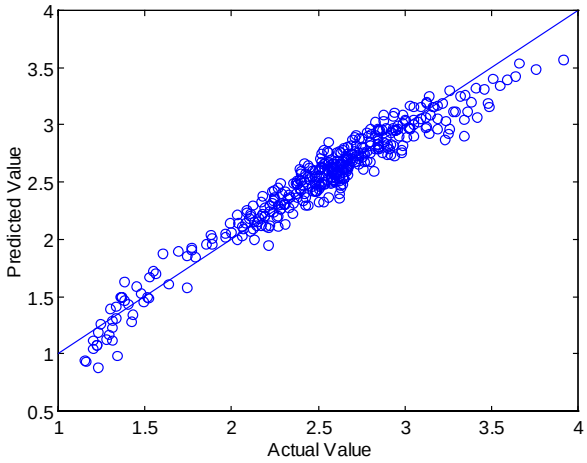

Figure 25. Instr 2: Calibration for Viscosity

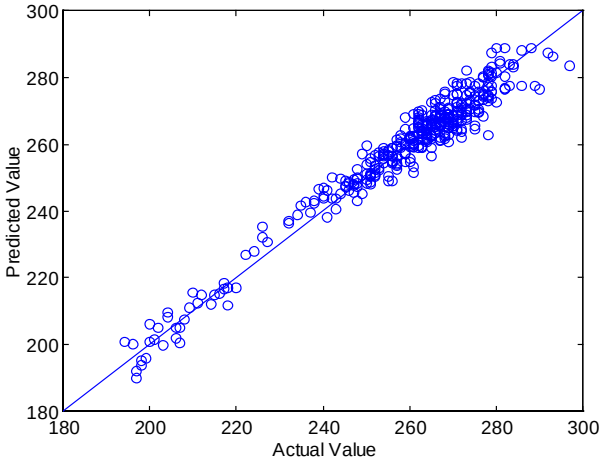

Figure 26. Instr 2: Calibration for BP50

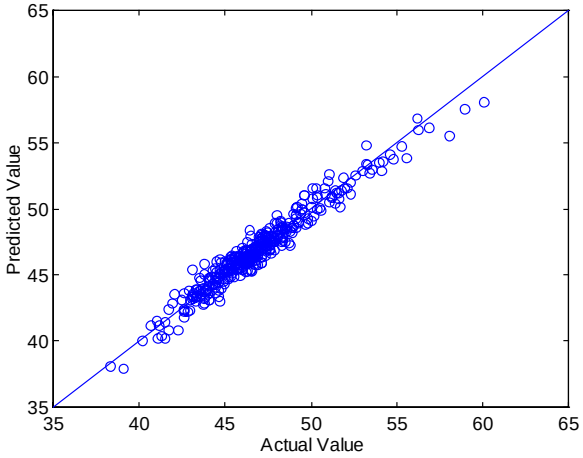

Figure 27. Instr 2: Calibration for Cetane Index (D4737)

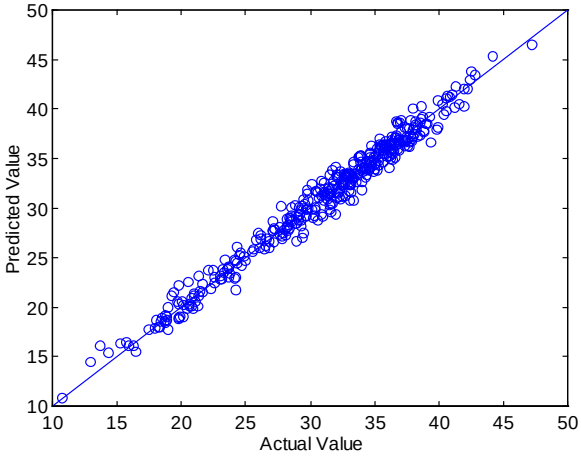

Figure 28. Instr 2: Calibration for Total ArH

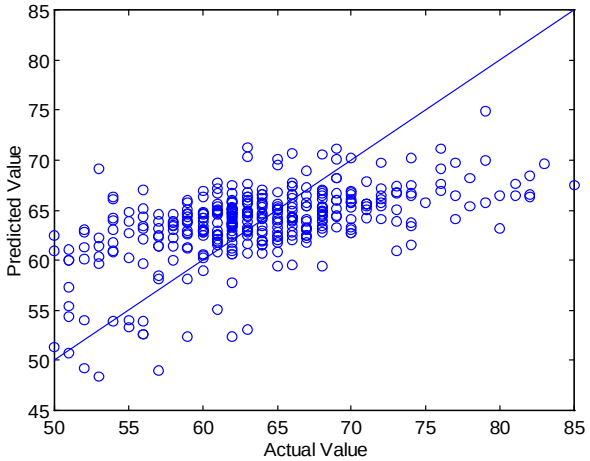

Figure 29. Instr 2: Calibration for Flash Point, Diesel Only

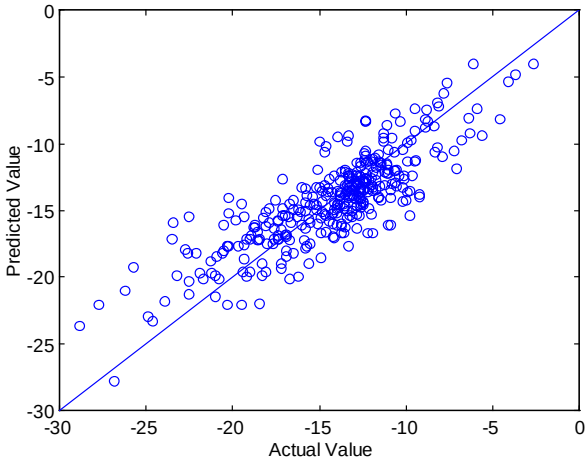

Figure 30. Instr 2: Calibration for Cloud Point, Diesel Only

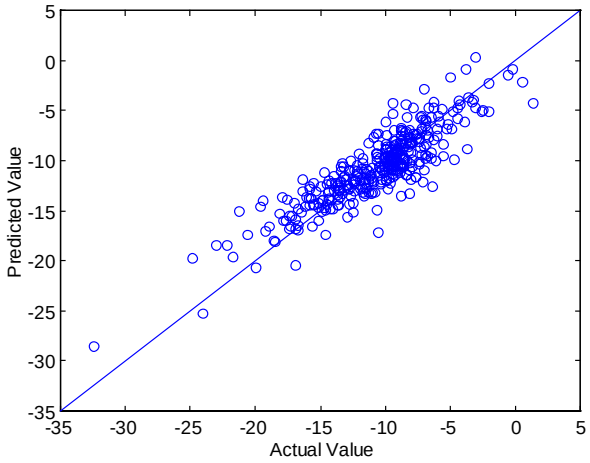

Figure 31. Instr 2: Calibration for Freeze Point, Diesel Only

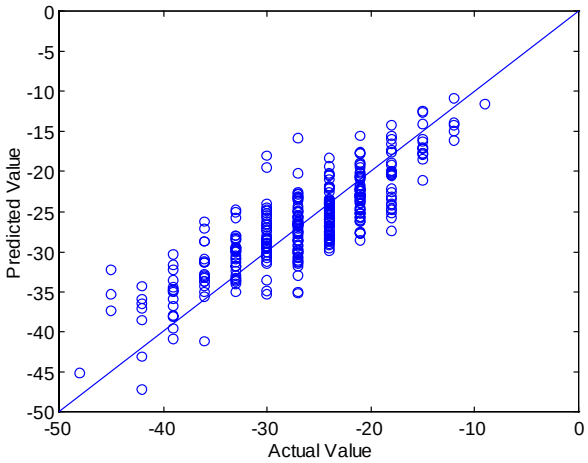

Figure 32. Instr 2: Calibration for Pour Point, Diesel Only

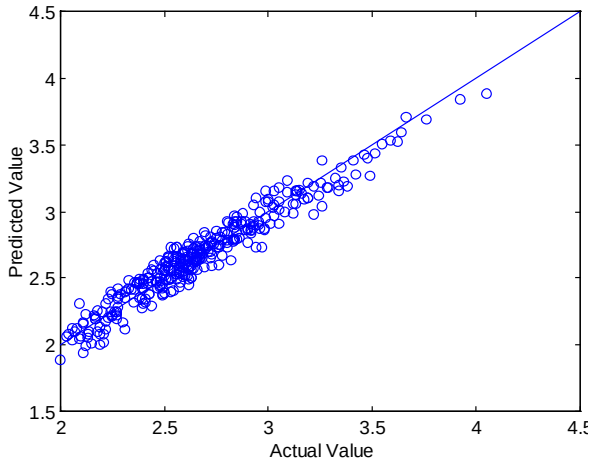

Figure 33. Instr 2: Calibration for Viscosity, Diesel Only

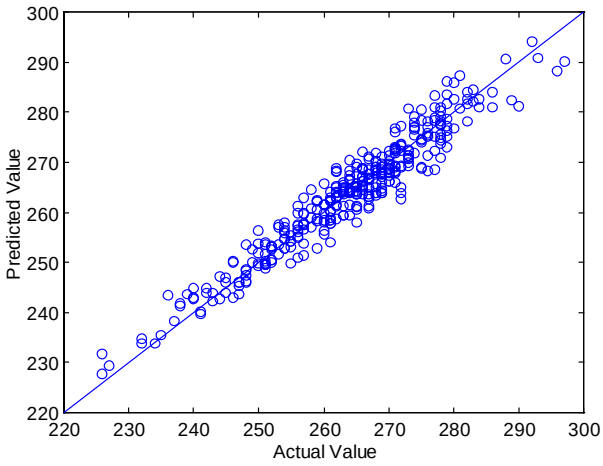

Figure 34. Instr 2: Calibration for BP50, Diesel Only

Table 10
Instrument 2, Diesel Only, PLS Calibrations,
First Difference/Mean-Centered

Property	Calibration Range Min.	Calibration Range Max.	SECV	SEP
Freeze	-32.4	1.4	2.4	3.3
Flash	50	85	6	6
Cloud	-28.8	-2.6	2.6	3.0
Pour	-48	-9	4	11
Viscosity	2.00	4.05	0.14	0.17
BP50	226	297	5	6

6.3 Model Validation

Using the validation set of samples, the calibration models were validated to better assess their usefulness. Table 9 reports the *SEP* for the diesel fuel/kerosene models. Predicted *vs.* Actual validation plots for density, cloud point, viscosity, BP50, CCI4737, and total aromatics are shown in Figures 35-40, respectively. The remainder of the validation plots are given in Appendix A, Figures 17-32. The MD for each validation sample was calculated and used to detect possible outliers. Those samples with D^2 D^2_{max} were excluded from the validation plots and the *SEP* calculation.

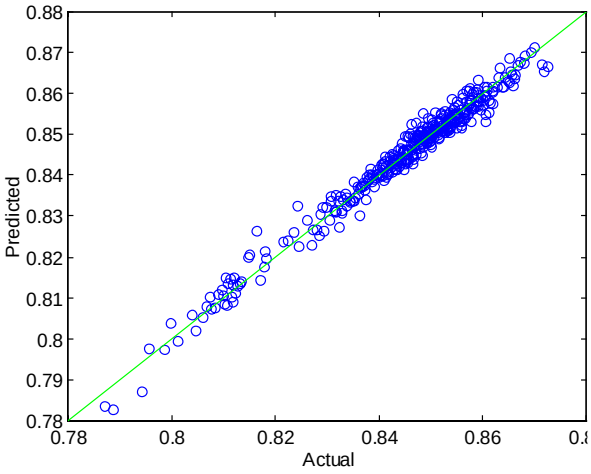

Figure 35. Instr. 2: Validation for Density

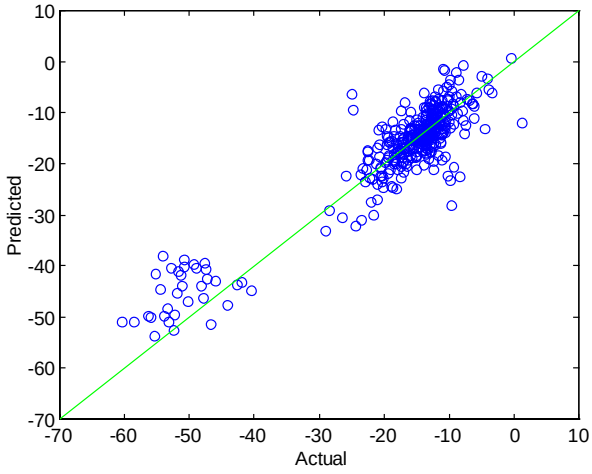

Figure 36. Instr. 2: Validation for Cloud Point

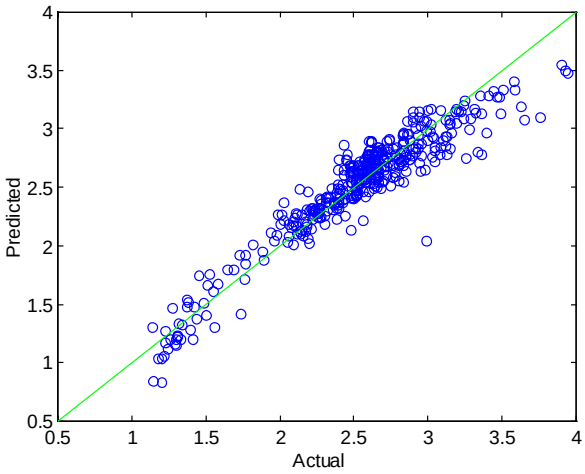

Figure 37. Instr. 2: Validation for Viscosity

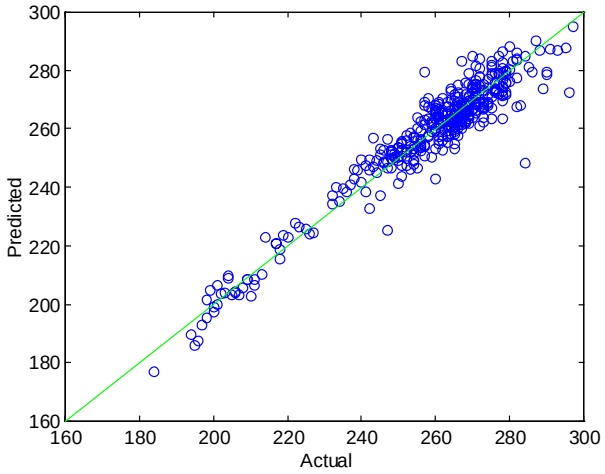

Figure 38. Instr. 2: Validation for BP50

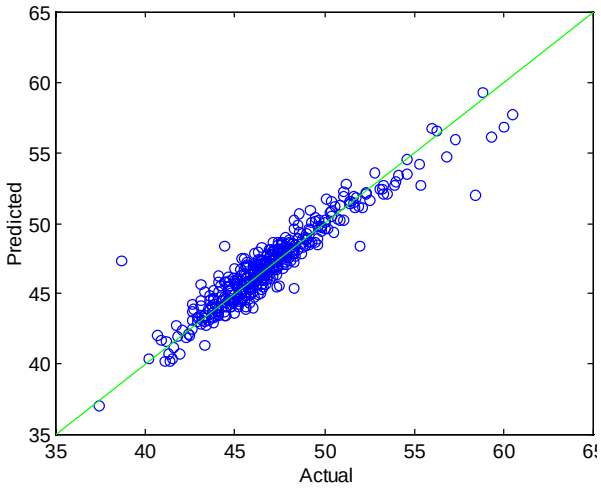

Figure 39. Instr. 2: Validation for Cetane Index (D4737)

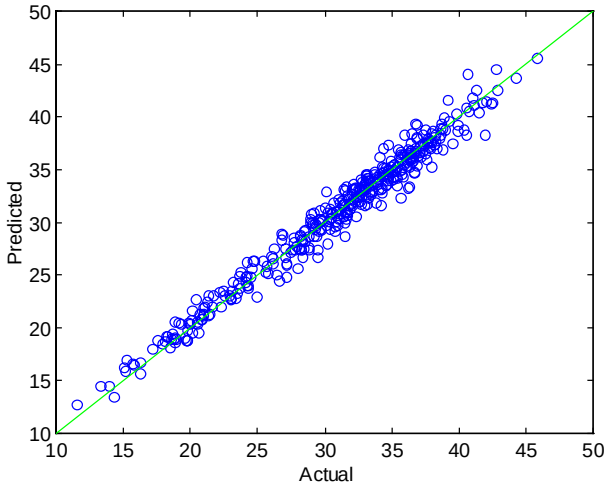

Figure 40. Instr. 2: Validation for Total ArH

To assess the validity of the models, Equation 8 was applied to each of the properties to determine the percentage of the reference values that fell within the specified interval (predicted value ± reproducibility). As shown in Table 9, models for viscosity, aromatics (mono, di, tri, total), net heat of combustion, hydrogen content, carbon content, and cetane index (D 4737 and D 976) were considered acceptable (i.e., 95% of the reference values fell within the interval specified by Equation 8). Interestingly, most of these properties are strongly related to the relative ratios of aliphatic and aromatic character in the sample as discussed in Section 2.5. Since the aromatic character shows a strong presence in the near-infrared spectra of fuel, this may lead to improved models for those properties.

Even with the large reproducibility values specified for the distillation properties in Table II, none were considered acceptable. Boiling points are obviously difficult to reproduce. Typically, BP50 should give the best correlation because at that point the distillation has stabilized and the distillate from each sample has similar characteristics. However, because of the wide compositional differences in fuels, the extremes of the distillation range vary widely and the boiling point becomes difficult to pinpoint. Indeed, of all the boiling points BP50 was found to be the best model, showing 92.6% inclusion of the reference values in the interval specified by Equation 8.

Flash point was also found to be poor at only 43.0% inclusion. There is a reasonable explanation for this based on how the samples were handled. Typically, the fuels arrived at the lab in 1 gallon cans. Enough fuel was taken from these cans to run the lab analyses and the remainder of the fuel was placed in cold

storage. Since the fuel sample was inevitably opened and closed on many occasions during the lab analyses, some of the highly volatile species would have been lost. Therefore, the sample that was used to run the ASTM flash point test may be significantly different than the sample used to collect the spectra simply by loss of these volatile species. Each time the sample container is opened and closed, the volatile species that collect in the headspace above the fuel would escape. The flash point is linked to the most volatile species and their loss would change the flash point of the fuel. Another possibility is that the volatile species that are responsible for the flash point are in such low concentrations that the near-infrared instrument is simply not sensitive enough to detect and/or resolve them.

Cloud point (73.1%), freeze point (51.8%), and pour point (45.9%), were all found to be poor, based on Equation 8. The *SEP* for pour point was especially poor compared to its *SECV* for the model. This indicates that the model is sufficiently poor that it cannot account for the small variations seen in the validation set samples. There are two possible problems with pour point. First, pour point data is collected in increments of 3°C, which may not be precise enough for accurate correlation to the near-infrared spectra (*i.e.,* the error in the reference method is large). Second, pour point suppressants are commonly added to fuel in low ppm levels. While these additives greatly affect the pour point, their concentration is below the detection limit of the near-infrared spectrometer. Therefore, the calibration models lack this additional variation necessary to model pour point correctly. Similarly, cloud point is defined as the temperature at which wax crystals begin to appear. The waxes are formed from high-molecular-weight paraffinic material present in very low concentrations and not detectable by the spectrometer.

The most surprising find was that the model for density gave the worst result of all at only 17% inclusion. Based on the low reproduciblity value, R=0.0005, density was expected to give one of the better models. However, based on our findings a hypothesis was formulated to account for the seemingly poor results for density. When constructing a calibration model, emphasis is often placed on improving the accuracy and precision of the reference method. This is done believing that as the reference measurements get better, so will the models. In fact, it may be possible that at some point the precision of the reference method may exceed its usefulness. The amount of information that can be extracted from the spectra must also be considered. Considering the relatively poor resolution and peak separation in near-infrared spectra, it may be possible that the limiting factor in the density model is not the reference method but

the spectra. Despite the results shown here, the model for density is believed to be sufficient. Many suppliers only report density to the third decimal place; the implication is that the extra precision is not needed. Given the *SEP*=0.0024 (Table 9), this model can estimate a fuel's density to the same precision.

Using Equations 5-7, no statistically significant bias was found. The *t*-test was performed for three models: density (e_v=6.21×10^{-5}, *SDV*=0.0023, and *t*=0.53), total aromatics (e_v=0.02, *SDV*=1.06, and *t*=0.37), and pour point (e_v=-0.20, *SDV*=18, and *t*=-0.22). In all cases, the *t*-test gave *t* values less than the critical *t*, t_c=1.96. Also, the fact that *SDV*≈*SEP* (Table 9) for each further shows a lack of significant bias.

Models built using only diesel were also validated (Table 10); outliers were not removed from these determinations. As seen in the *SECV*, *SEP* values for cloud and freeze point also improved. Figures 41-43 show Predicted *vs.* Actual for cloud, freeze, and pour points. Had outliers been removed, the *SEP* would be lower than reported. Although they appear promising, no further work has been done with these models. Without additional kerosene samples, attention must focus on developing models that accommodate both fuel types.

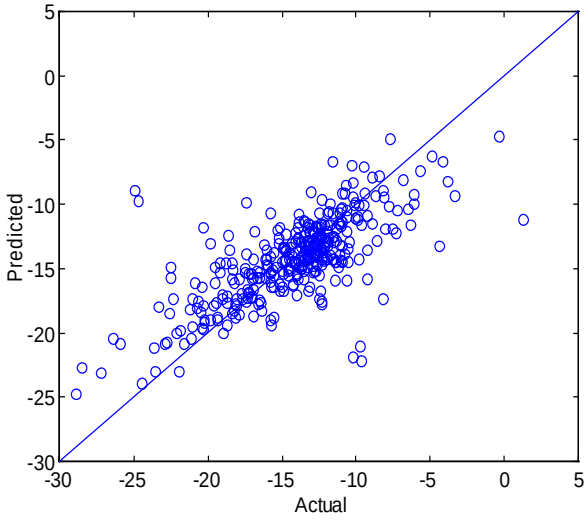

Figure 41. Instr. 2: Validation for Cloud Point, Diesel Only

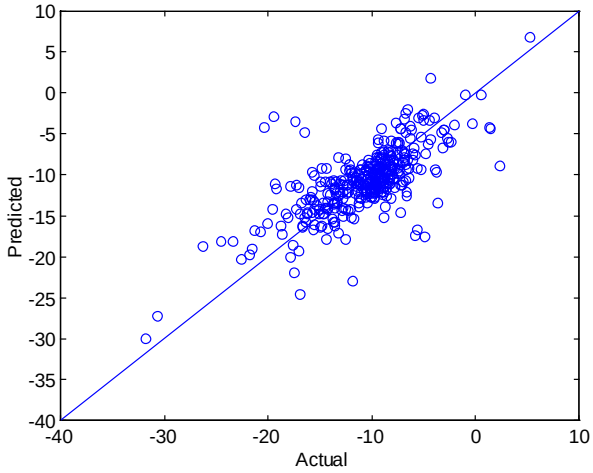

Figure 42. Instr. 2: Validation for Freeze Point, Diesel Only

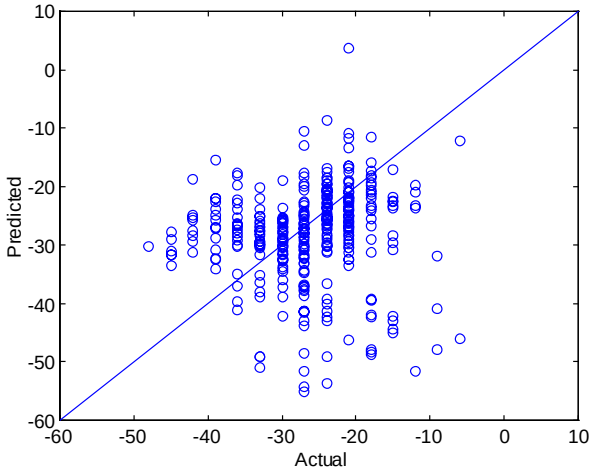

Figure 43. Instr. 2: Validation for Pour Point, Diesel Only

6.4 Summary

Based on a 95% confidence interval (Equation 8), viscosity, cetane index, net heat of combustion, aromatics, carbon content and hydrogen content were determined to have acceptable models for estimating diesel fuel and kerosene properties in this application. Although shown to be statistically poor by the same statistic, the models for density and BP50 should also be sufficient as explained above. Comparison of SEP values showed that cloud point and freeze point could also yield acceptable results when using models constructed solely for diesel fuel. This area will be pursued once additional kerosene samples can be obtained. The results for the remainder of the boiling point models were found to be insufficient for our application. In general, all of the models constructed can provide rough property estimates, but the decision to use them ultimately lies with the end user and his/her application. The criteria that has been set for acceptance may be too stringent for some and too lenient for others. Many of the models lack sufficient accuracy to be useful in more critical applications (e.g., for aircraft fuel).

7.0 CALIBRATION TRANSFER

7.1 Preliminary Investigations of Calibration Transfer

Experiments for calibration transfer were carried out approximately one year after the original calibration spectra had been collected. During that year, both Instruments 1 and 2 had been modified with some minor repairs and upgrades. The purpose of this experimentation was to determine if the models created with spectra from Instrument 2 in its original state could be applied to spectra currently being collected.

Spectra for the five reference fuels were collected on Instrument 2, and the diesel/kerosene models for density, total aromatics, cetane index (ASTM D 4737), and viscosity were applied. The *SEP*, shown in Table 11, was calculated for each property to provide a cursory measure of comparison with the calibration transfer results. Comparing the *SEP*s in Table 9 with those in Table 11 shows the adverse effects that the elapsed time and hardware modifications had on the calibrations. The results became essentially useless.

Table 11
Instrument 2, Reference Fuel Predictions
No Calibration Transfer

Property	SEP
Density	0.0309
Total ArH	11.8
CCl4737	2.0
Viscosity	2.94

An empirical approach was taken to find suitable conditions with which to perform the calibration transfer. Twenty methods, shown in Table 12, were chosen to allow variations in both the window size and the number of spectra to be tested. Methods 1-4 use PDS and method 5 uses DS. Each method was run with and without the additive background correction.

Table 12
Calibration Transfer Methods

Method Number	Window Size	Number of Spectra
1.1	11	3
1.2	11	5
1.3	11	7
1.4	11	9
2.1	51	3
2.2	51	5
2.3	51	7
2.4	51	9
3.1	101	3
3.2	101	5
3.3	101	7
3.4	101	9
4.1	151	3
4.2	151	5
4.3	151	7
4.4	151	9
5.1	0	3
5.2	0	5
5.3	0	7
5.4	0	9

Calibration transfer protocols, without background correction, were generated for each method using first difference spectra and applied to the reference spectra for Instrument 2. The original models for density, total aromatics, cetane index (ASTM D 4737), and viscosity were used to estimate the property values of the transformed reference spectra. The *SEP* was calculated for each method and property and is shown in Tables 13 and 14 for PDS and DS, respectively. The same treatment was carried out in generating the transformations with the additive background correction added to the transformed spectra. Those results are shown in Tables 15 and 16 for PDS and DS, respectively. Inspecting Tables 13-16, it became obvious that DS, with or without background correction, gave inferior results to PDS as expected. Further comparison of Tables 13 and 15 led to the empirical selection of method 3.2 (without background correction) as the most suitable transfer method. This method gave the lowest *SEP* for both density and total aromatics out of all the methods tried. The *SEP*s for viscosity and cetane index were slightly higher than other methods but were still considered usable.

Table 13
SEP for Calibration Transfer using Piece-Wise Direct Standardization
No Background Correction. Instrument 2 to Instrument 2.

Method	Density	Total ArH	CCI4737	Viscosity
1.1	0.0103	3.1	1.8	0.63
1.2	0.0083	2.5	3.9	0.75
1.3	0.0081	2.1	3.7	0.59
1.4	0.0088	2.2	3.9	0.62
2.1	0.3529	8.8	21.2	0.43
2.2	0.0033	1.4	2.2	0.22
2.3	0.0046	0.9	2.6	0.24
2.4	0.0060	1.6	2.5	0.38
3.1	0.0217	11.9	7.0	0.28
3.2	0.0025	0.6	3.3	0.20
3.3	0.0039	0.9	3.2	0.16
3.4	0.0050	1.9	2.8	0.29
4.1	0.0265	12.5	6.0	0.22
4.2	0.0061	1.1	4.0	0.51
4.3	0.0080	0.7	2.9	0.30
4.4	0.0079	1.0	3.4	0.47

Table 14
SEP for Calibration Transfer using Direct Standardization
No Background Correction. Instrument 2 to Instrument 2.

Method	Density	Total ArH	CCl4737	Viscosity
5.1	0.0294	13.1	3.7	0.63
5.2	0.0132	6.4	4.8	0.65
5.3	0.0046	1.3	3.9	0.27
5.4	0.0063	1.8	4.2	0.58

Table 15
SEP for Calibration Transfer using Piece-Wise Direct Standardization
Background Corrected. Instrument 2 to Instrument 2.

Method	Density	Total ArH	CCl4737	Viscosity
1.1	0.0101	5.3	1.3	0.50
1.2	0.0052	2.9	2.0	0.41
1.3	0.0066	3.4	6.0	0.43
1.4	0.0098	60.8	4.0	0.65
2.1	0.0046	60.8	46.1	0.86
2.2	0.0046	2.8	1.8	0.28
2.3	0.0038	1.6	3.1	0.21
2.4	0.0034	1.4	4.4	0.48
3.1	0.0140	56.8	47.1	0.84
3.2	0.0046	2.7	1.8	0.29
3.3	0.0048	1.6	3.4	0.30
3.4	0.0054	1.6	4.0	0.62
4.1	0.0462	56.3	46.1	1.12
4.2	0.0083	3.6	2.8	0.46
4.3	0.0065	2.0	4.1	0.39
4.4	0.0063	1.8	4.3	0.60

Table 16
SEP for Calibration Transfer using Direct Standardization
Background Corrected. Instrument 2 to Instrument 2.

Method	Density	Total ArH	CCl4737	Viscosity
5.1	0.0214	56.2	43.8	1.49
5.2	0.0123	6.0	4.7	0.63
5.3	0.0073	1.8	4.2	0.38
5.4	0.0087	1.8	4.5	0.57

One last calculation was carried out to determine the effectiveness of the calibration transfer to correct the MD for the newly run reference spectra. Table 17 shows the MD, with and without calibration transfer, using method 3.2 (without background correction). The D^2_{max} for Instrument 2 was 0.1559. Without the benefit of the calibration transfer, all of the samples would have been flagged as outliers. With the correction provided by the calibration transfer, only one sample exceeds the recommended D^2_{max} limit. In essence, the calibration transfer protocol has made the recently run reference spectra appear as if they were run back near the time when the calibration spectra were originally collected.

Table 17
Instrument 2: Effect of Calibration Transfer on Mahalanobis Distance (MD)

Reference Sample Number	MD without Calibration Transfer	MD with Calibration Transfer (Method 3.2)
24792	2.75	0.05
24793	2.96	0.36
24794	3.05	0.07
24795	3.05	0.05
24508	3.90	0.14

7.2 Conclusions

As was expected, PDS provided the best results. While the results were encouraging, there is some concern that, ultimately, maintaining the integrity of even a few representative fuel samples over an extended period may prove to be impossible. Alternative methods for maintaining the calibration models will need to be identified and investigated. However, further investigations of calibration transfer have not been attempted to date. The fact that an additive background was not needed was not surprising since the routine for collecting spectra included a new background between each sample.

8.0 SUMMARY AND CONCLUSIONS

Near-infrared spectroscopy combined with chemometrics was explored as a viable solution to the military's need for a rapid means of identifying and analyzing fuels in the field. Calibration models were developed for a wide array of fuel properties for both diesel fuel and kerosene. At the present state of

development, the following models provide results that are acceptable for this application: density, viscosity, net heat of combustion, carbon content, hydrogen content, aromatic content (mono, di, tri, total), boiling point at 50% recovery, and cetane index. While some of the models (e.g., cloud point and freeze point) failed to meet the acceptance criteria, they were still able to provide rough approximations that may still be appropriate for some applications. Based on comparison of the SEP values, models for cloud point and freeze point that incorporated only diesel fuel appeared to yield better results than the combined diesel fuel and kerosene set. Again, these conclusions are based on the criteria required for the current application. Other than the general calibration procedure, there are no strict guidelines that must be adhered to when building calibration models. Users must generate their own criteria for determining whether a model is usable for their application. This application only involves determining a pass/fail result for a given sample. Therefore, the criteria for allowing the use of a calibration model need not be highly restrictive. In addition to constructing calibration models, outlier detection, discriminant analysis, and calibration transfer were also investigated with good success. This work represents a foundation for which future investigations can be compared.

As a result of this work, several observations were made that can be used to direct similar work in the future. PCA was found to be an indispensable tool for exploratory data analysis. Using scores plots, PCA can be used to visualize a data set and inspect it for irregularities or clustering that may not be obvious to the naked eye. Using standard solvents in conjunction with PCA to track instrument performance was also found to be useful. However, while the solvents are suitable for a laboratory environment, they might be difficult to maintain in the field. Rather than using liquid standards, solid standards (e.g., polystyrene) may be more appropriate for a field setting. The solid standards could be used in conjunction with the calibration transfer techniques to update the calibration data for the instrument.

A significant disadvantage of the near-infrared spectrometers used in this study was the lack of instrument diagnostics. Additional measures had to be taken to ensure that the instrument was performing as expected. Mahalanobis Distance (MD) was one method investigated to determine a sample's potential to be an outlier. At the current time, MD is the only method being used. However, since MD is sensitive to changes in the spectra it could be difficult to tell whether a potential outlier is truly a bad fuel sample or if the instrument is not functioning properly. Another possibility would be to

track the performance of a standard with known property values. The standard should not be a fuel because fuels will degrade and they cannot be replaced to the same specification. Instead, a solvent or solid standard could be used to create a trend of instrument performance where drift would be noticeable.

Discriminating diesel fuel from kerosene and gasoline was accomplished successfully. Using a simple 2-point Euclidean-based measure provided satisfactory separation of diesel fuel and kerosene from gasoline. Separating diesel fuel from kerosene is also possible using the net heat of combustion and could be modified to include additional properties like density. Eventually, more kerosene samples and a large set of gasolines will need to be acquired so that separate calibration models can be constructed for each. The results obtained from the calibration transfer work were very encouraging. Spectra being collected more than one year from when the calibration models were constructed were estimated satisfactorily. However, calibration transfer does pose one problem. Trying to maintain a small representative set of the original calibration samples indefinitely will not succeed, and new samples will have to be acquired. The use of solid standards (e.g., glass filters, neutral density filters) or liquid standards (i.e., solvents) may need to be investigated as an alternative to fuels for calibration transfer. Rather than use calibration transfer, one could also calculate and apply a bias correction (an offset) to each model periodically to help maintain its accuracy. However, without the transformation supplied by the calibration transfer, the discriminant analysis and Mahalanobis Distance calculation will ultimately fail because these methods rely on the spectra. This will be a difficult challenge to overcome before any instruments can be fielded. The best compromise may be to use both calibration transfer and a bias correction. A bias correction could be applied in the interim between rebuilding of the calibration transfer functions. This could prevent the instrument from being offline for more than 30 minutes at a time when its use is critical. Once the instrument is removed from deployment, a new calibration transfer could be constructed.

An issue not investigated in this work was that of calibration transfer between *different* instruments. Using the same methods applied in this work for updating an instrument, a calibration model can also be transferred to a different instrument. This becomes useful when a series of instruments must be fielded. Instead of running all of the samples on each of the instruments, the samples can be run once, on one instrument. The models built on that instrument can then be transferred to each of the instruments with

minimal effort and expense. Based on the results of this work, calibration transfer between different instruments should be feasible. However, additional factors that may affect the results include the type of sampling accessory used (e.g., probe vs. cuvette), a shift in wavelength position, relative amounts of noise in the spectra, and spectra of different resolution.

At the present time, the following properties are being considered for use in the field: density, total aromatics, kinematic viscosity, net heat of combustion, and cetane index. These properties provide the most useful information about a fuel and its suitability for consumption. Additional properties are available, such as cloud point and 50% boiling point, provided that the degree of accuracy is acceptable. For use in the field, limits can be set to determine a pass/fail decision for a given fuel. These limits can be based on an actual fuel specification or specifications that are believed to be appropriate. Table 18 shows an example of what the limits might look like. In the table, pass means that the fuel falls within the optimum range expected for that fuel property. An acceptable rating means that the fuel property is slightly higher or lower than expected for that fuel but should not affect the use of the fuel. However, it serves as a warning that something is causing or has caused the fuel property to change. Fail means that the fuel is outside the range allowed by that fuel's specification. The use of the acceptable rating requires some knowledge of the fuel being used and scrutiny in how the limits are set.

Table 18
Limits for Fuel Property Estimates

Property	Fail	Acceptable	Pass	Acceptable	Fail
Density at 15°C, g/mL	<0.7700	<0.8000	0.8000-0.8600	>0.8600	>0.9100
Viscosity at 40°C, cSt	<0.9	<1.3	1.3-3.9	>3.9	>4.5
Cetane Index	<35	<40	40-55	>55	>70
Total ArH, mass %	<5	<10	10-50	>50	>60
Net Ht. of Comb., MJ/kg	<41	<42	42-43	>43	>45

Overall, the work was accomplished successfully. At the present time, work is underway to reduce the size of the related hardware, to include other fuel types (e.g., gasoline), and to investigate other fuel properties.

9.0 REFERENCES

1. Burns, D.A.; Ciurczak, E.W., *Handbook of Near-Infrared Analysis*, Marcel Dekker, Inc., New York., 1992.
2. Luminar 2000 NIR Spectrometer Manual V2.3.1, Brimrose Corporation of America, 1995.
3. Brown, S.D. *Appl. Spectrosc.* **1995**, *49*, 14A-31A.
4. Thomas, E.V. *Anal. Chem.* **1984**, 66, 795A-804A.
5. Boldt, K.; Hall, B.R., *Significance of Tests for Petroleum Products*, ASTM, 1977.
6. Westbrook, S.R., Hutzler S.A., Interim Report TFLRF No. 313, U.S. Army TARDEC Fuels and Lubricants Research Facility (SwRI), Southwest Research Institute, San Antonio, Texas.
7. Fodor, G. E., Hutzler S. A., Interim Report TFLRF No. 321, U.S. Army TARDEC Fuels and Lubricants Research Facility (SwRI), Southwest Research Institute, San Antonio, Texas.
8. PLSplus IQ manual, Galactic Industries Corporation, 1996.
9. PLS_Toolbox manual, Eigenvector Research
10. Blanco, M.; Coello, J.; Iturriaga, H.; Maspoch, S.; de la Pezuela, C. *Appl. Spectrosc.* **1997**, *51*, 240-246.
11. Beebe, K.R.; Kowalski, B.R. *Anal. Chem.* **1987**, *59*, 1007A-1017A.
12. Haaland, D.M.; Thomas, E.V. *Anal. Chem.* **1988**, *60*, 1193-1202.
13. Geladi, P.; Kowalski, B.R. *Anal. Chim. Acta* **1986**, *185*, 1-17.
14. Martens, H.; Naes, T., *Multivariate Calibration*, John Wiley and Sons, Chichester, UK., 1989.
15. Mark, H.L. *Anal. Chem.* **1987**, *59*, 790-795.
16. ASTM Proposed Standard Practice for the Validation of Multivariate Process Infrared Spectrometers, 1996.
17. ASTM E 1655-97, Standard Practices for Infrared, Multivariate, Quantitative Analysis, 1995.
18. Blank, T.B.; Sum, S.T.; Brown, S.D., Montre, S.L. *Anal. Chem.* **1996**, *68*, 2987-2995.
19. Wang, Y.; Veltkamp, D.J.; Kowalski, B.R. *Anal. Chem.* **1991**, *63*, 2750-2756.
20. Wang, Y.; Lysaght, M.J.; Kowalski, B.R. *Anal. Chem.* **1992**, *64*, 562-564.
21. Chen, Chi-Shi, Brown, C.W., Lo, Su-Chin *Appl. Spectrosc.* **1997**, *51*, 744-748.
22. Wang, Z.; Dean, T.; Kowalski, B.R. *Anal. Chem.* **1995**, *67*, 2379-2385.

APPENDIX A
FIGURES

Figure 1. Instrument 2.
Calibration for Flash Point.

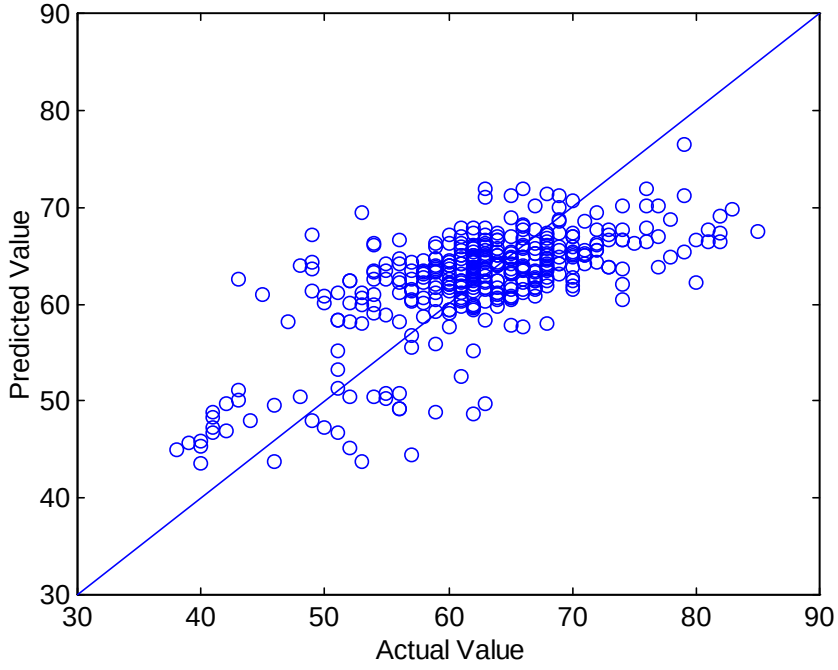

Figure 2. Instrument 2.
Calibration for Freeze Point.

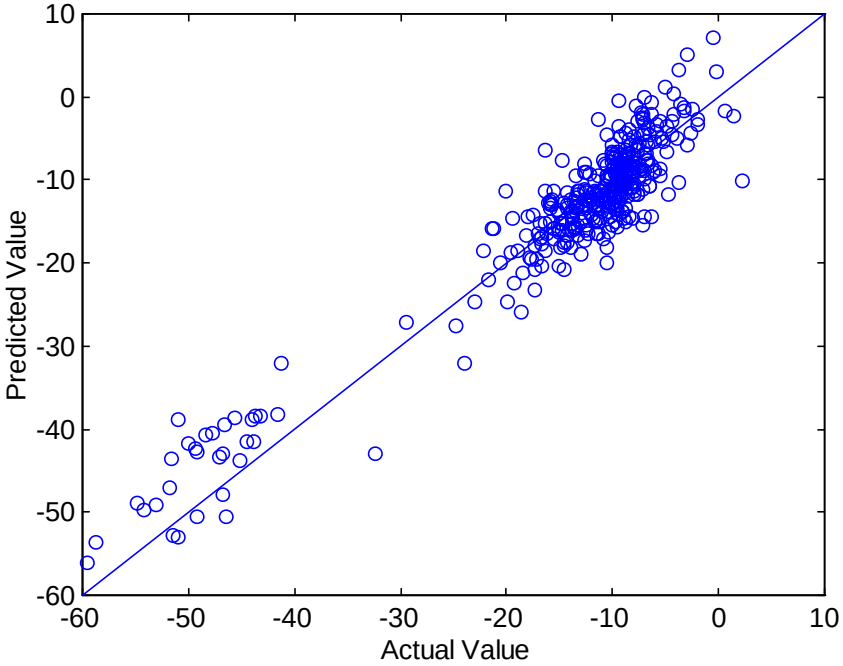

Figure 3. Instrument 2.
Calibration for Pour Point.

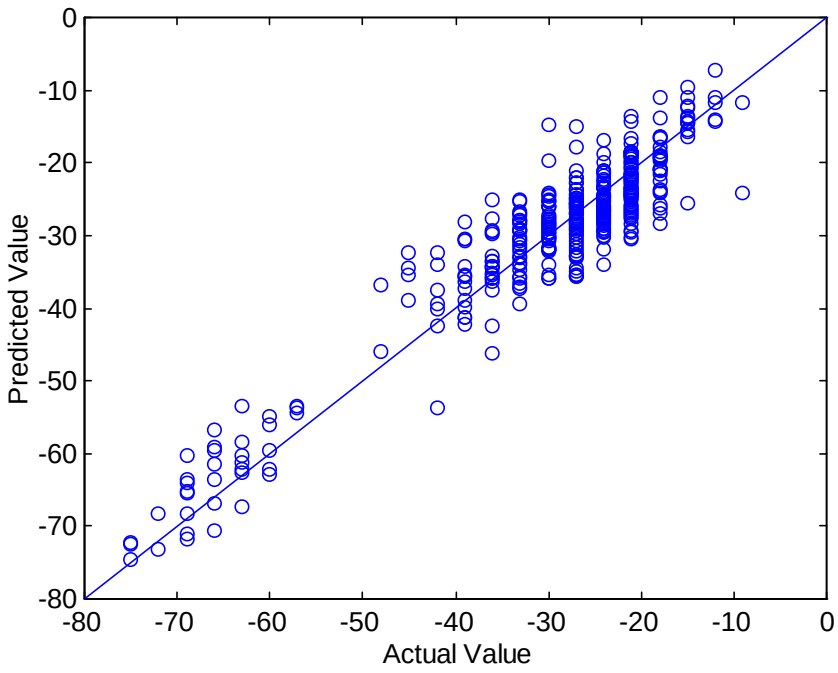

Figure 4. Instrument 2.
Calibration for IBP.

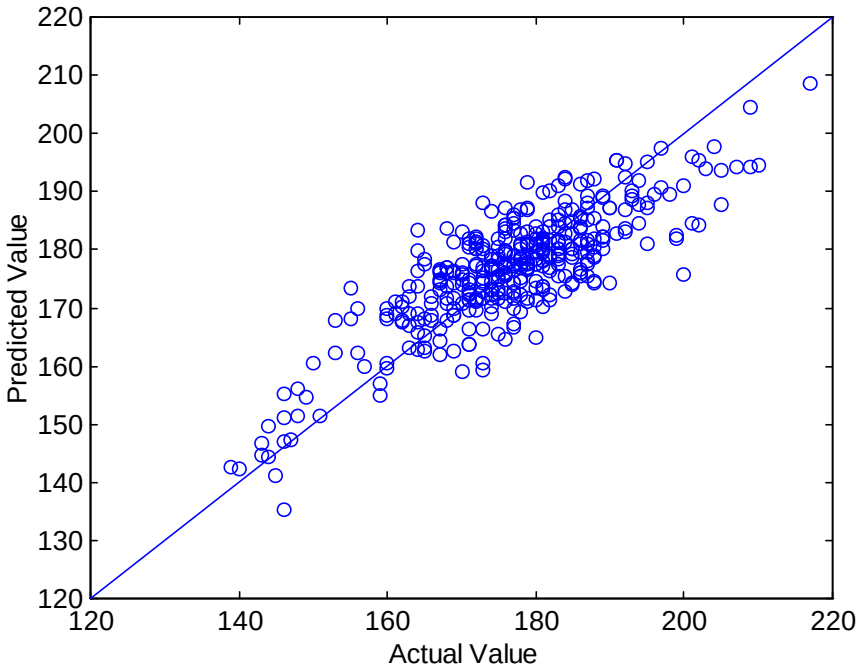

Figure 5. Instrument 2.
Calibration for BP10.

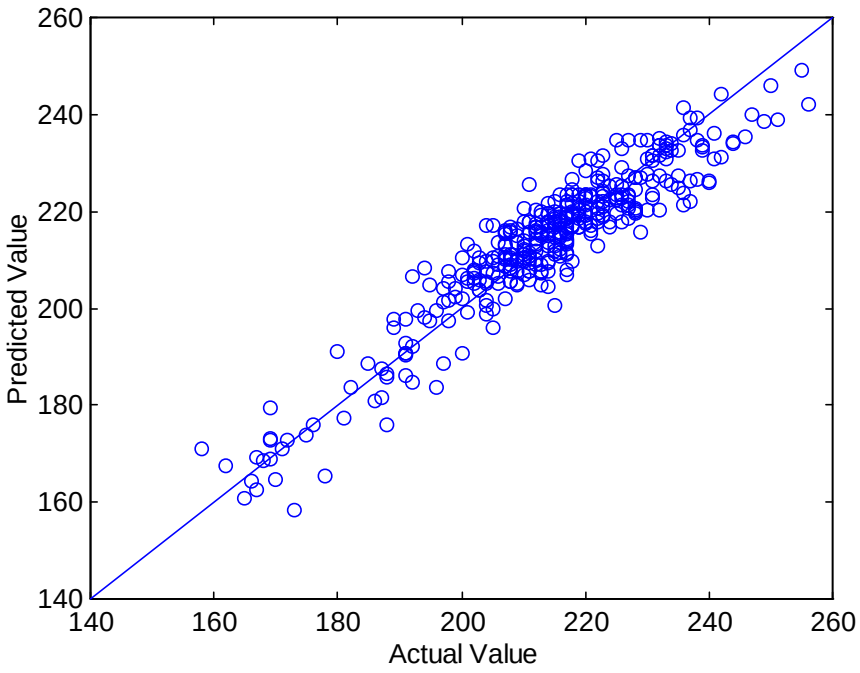

Figure 6. Instrument 2.
Calibration for BP90.

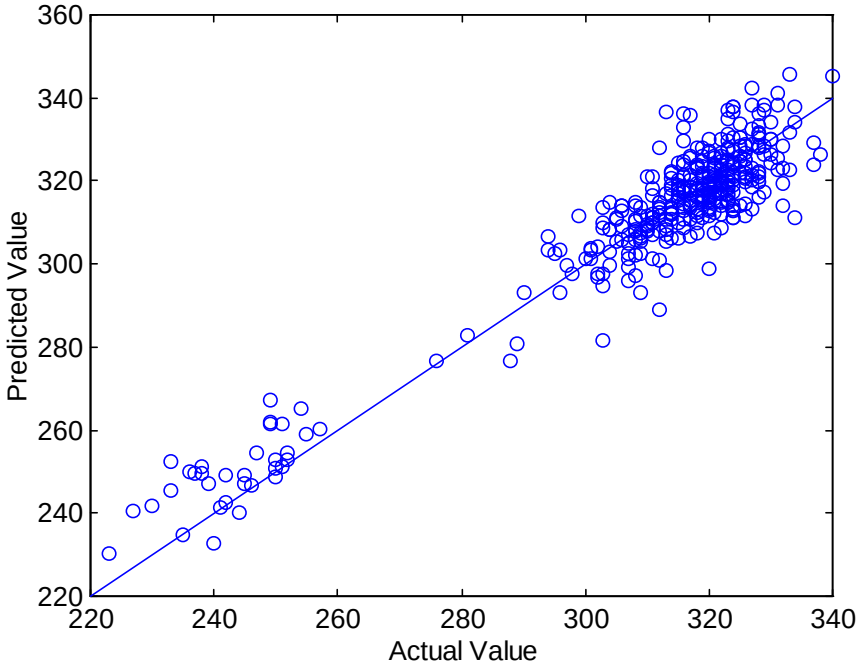

Figure 7. Instrument 2.
Calibration for BP95.

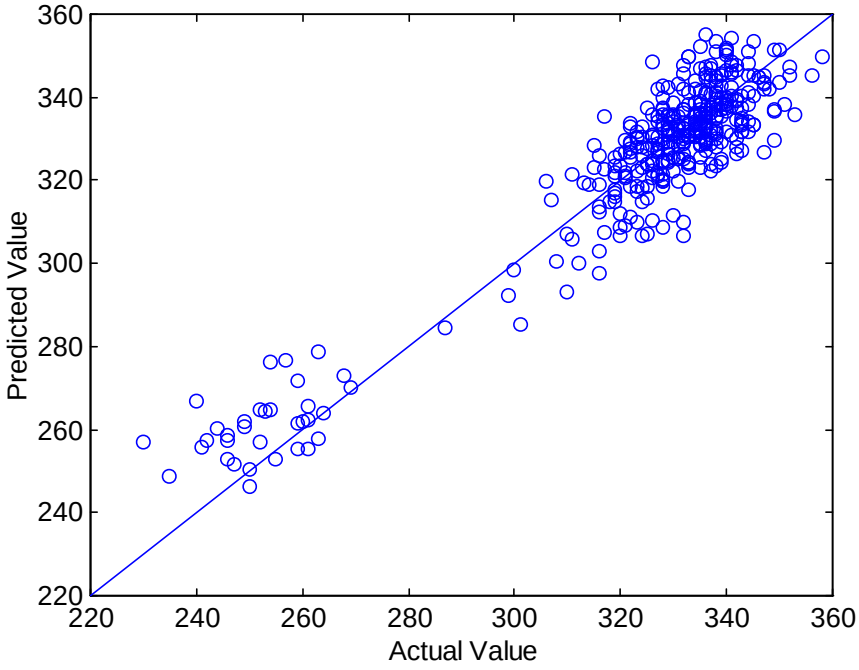

Figure 8. Instrument 2.
Calibration for BPEP.

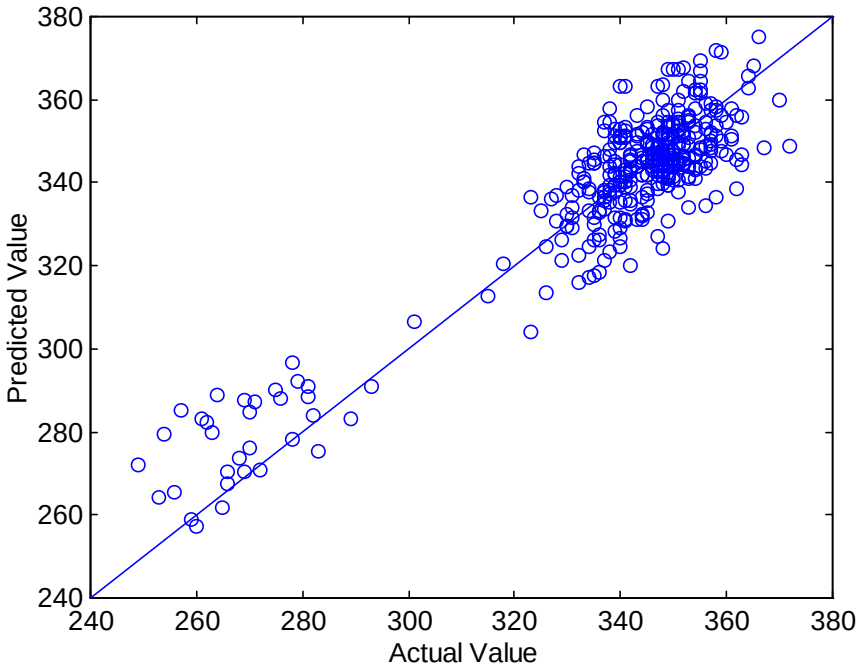

Figure 9. Instrument 2.
Calibration for Cetane Index (D976).

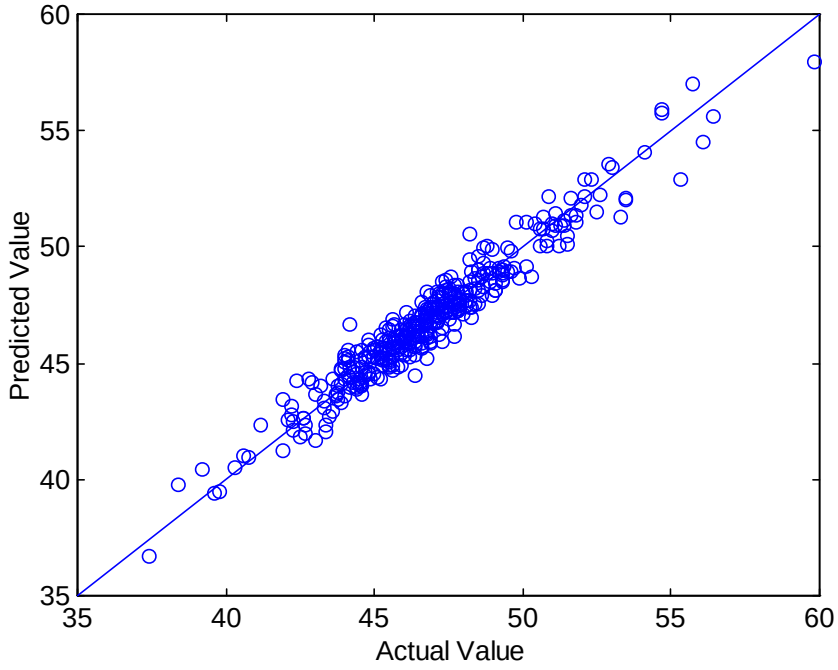

Figure 10. Instrument 2.
Calibration for Hydrogen Content.

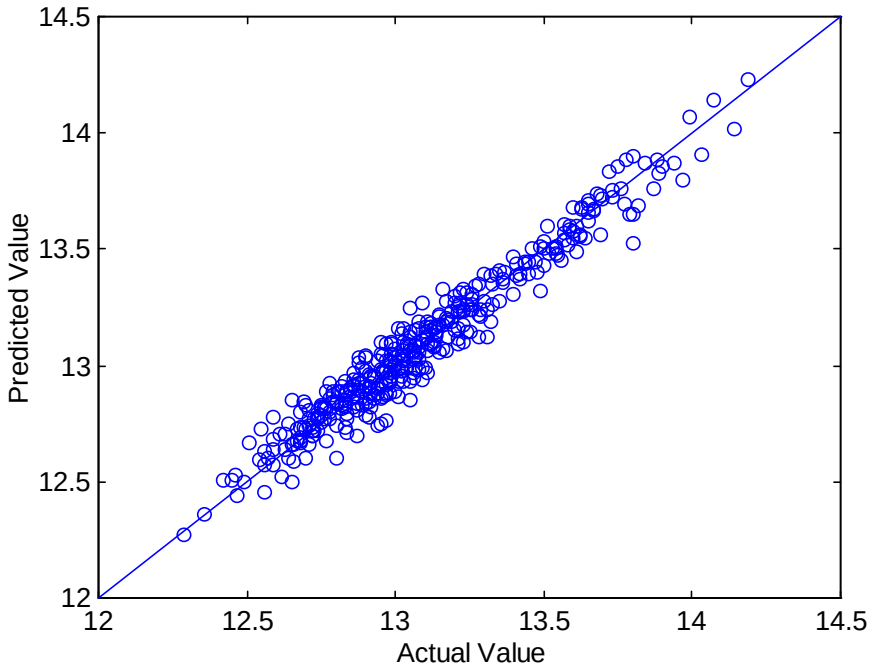

Figure 11. Instrument 2.
Calibration for Carbon Content.

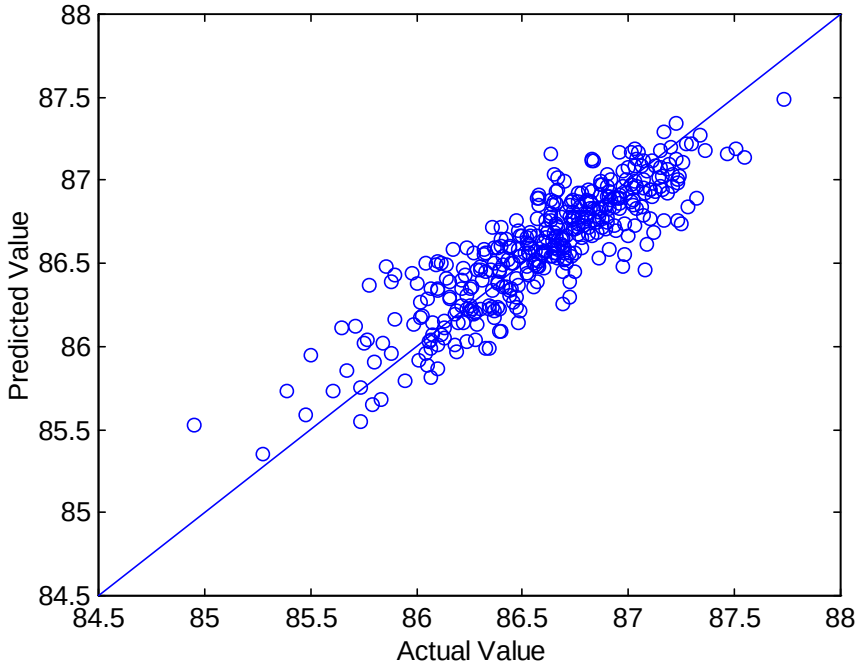

Figure 12. Instrument 2.
Calibration for Carbon/Hydrogen.

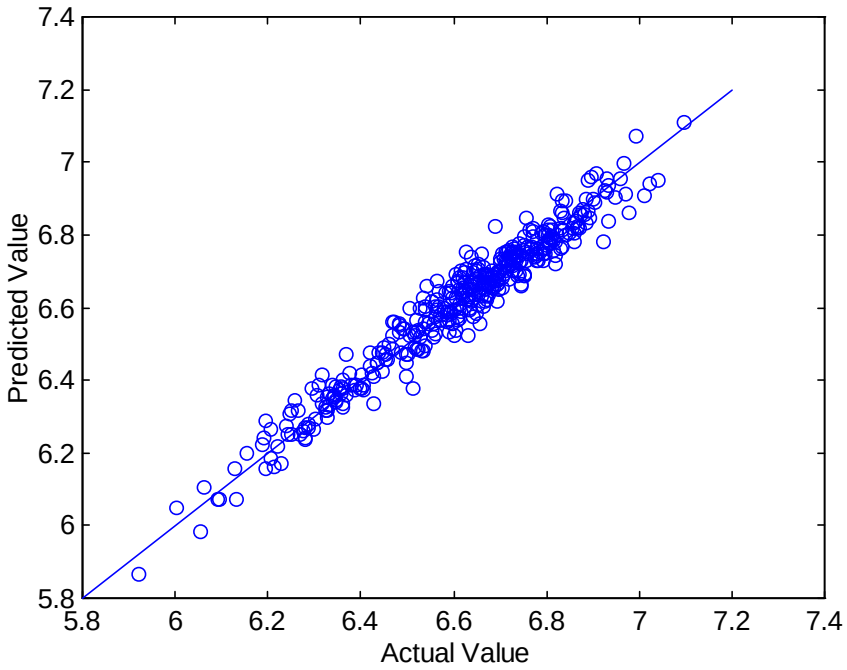

.

Figure 13. Instrument 2.
Calibration for NHC.

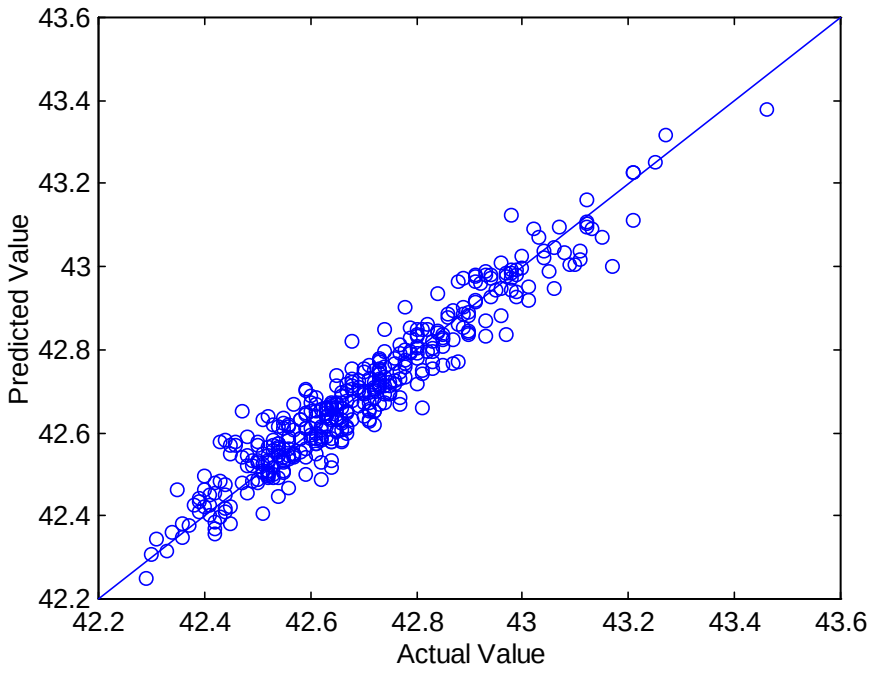

Figure 14. Instrument 2.
Calibration for 1-ArH.

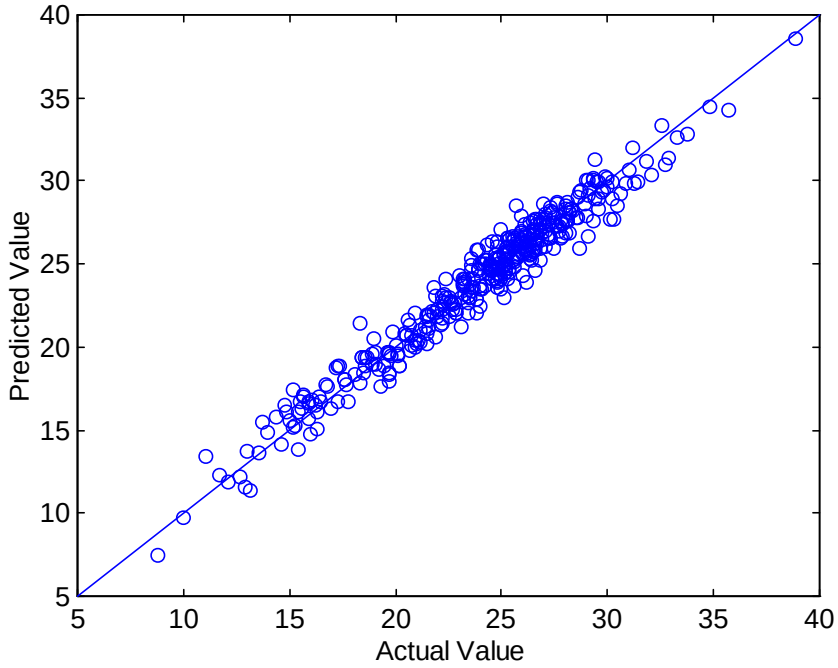

Figure 15. Instrument 2.
Calibration for 2-ArH.

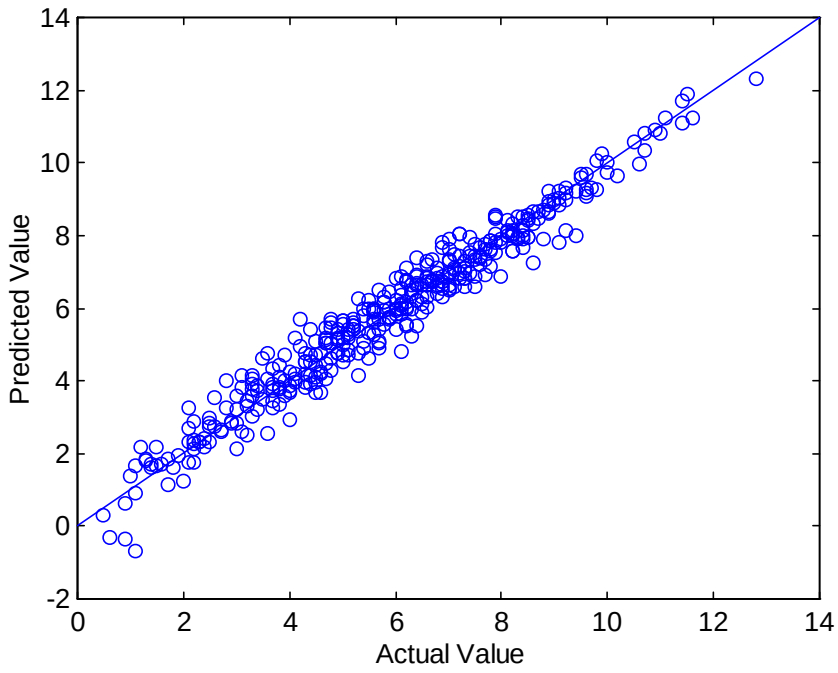

Figure 16. Instrument 2.
Calibration for 3-ArH.

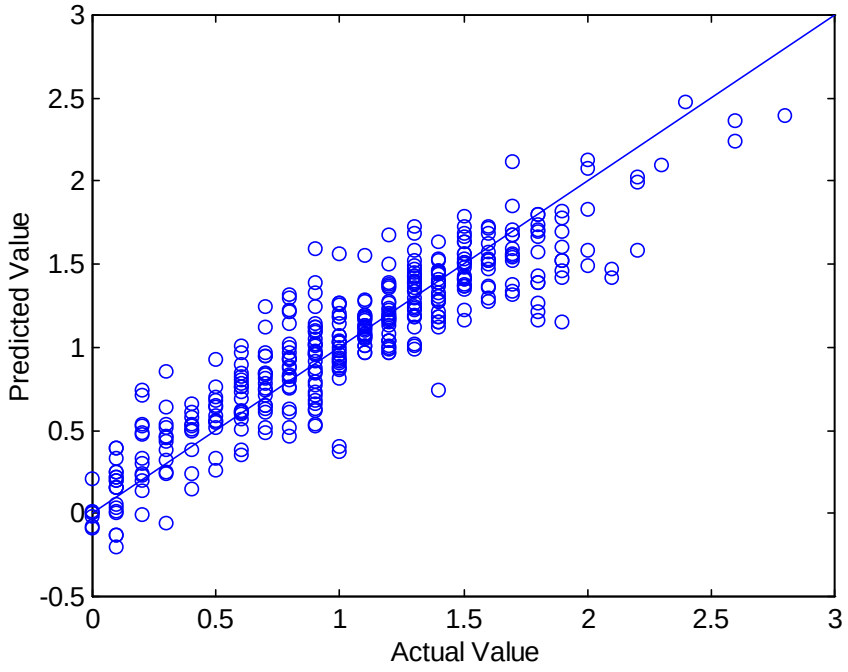

Figure 17. Validation for Flash Point.

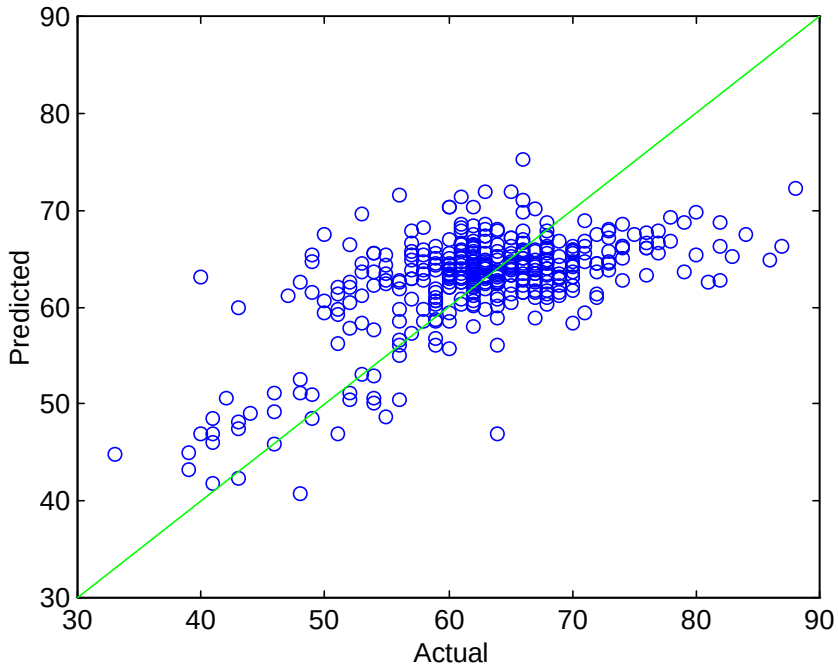

Figure 18. Validation for Freeze Point.

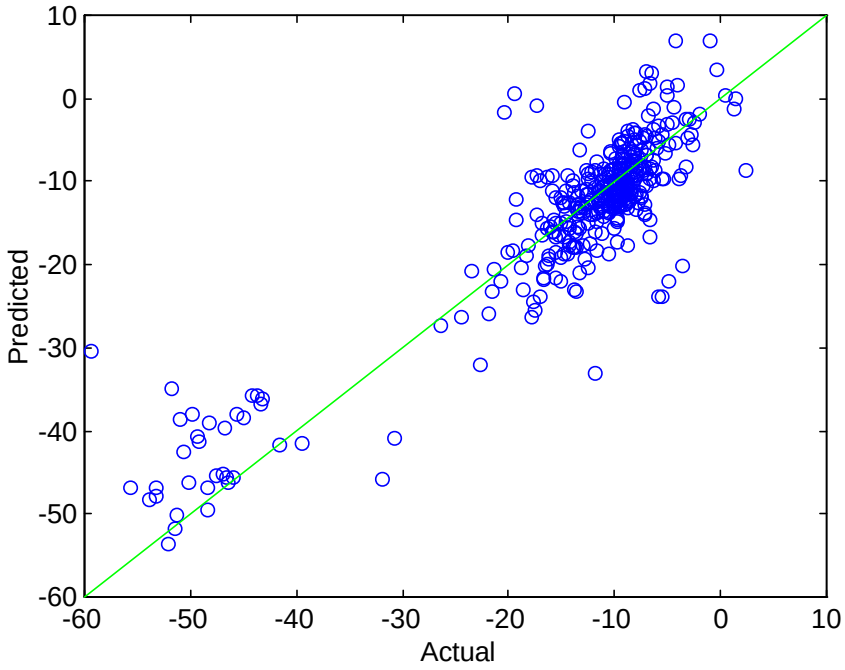

Figure 19. Validation for Pour Point.

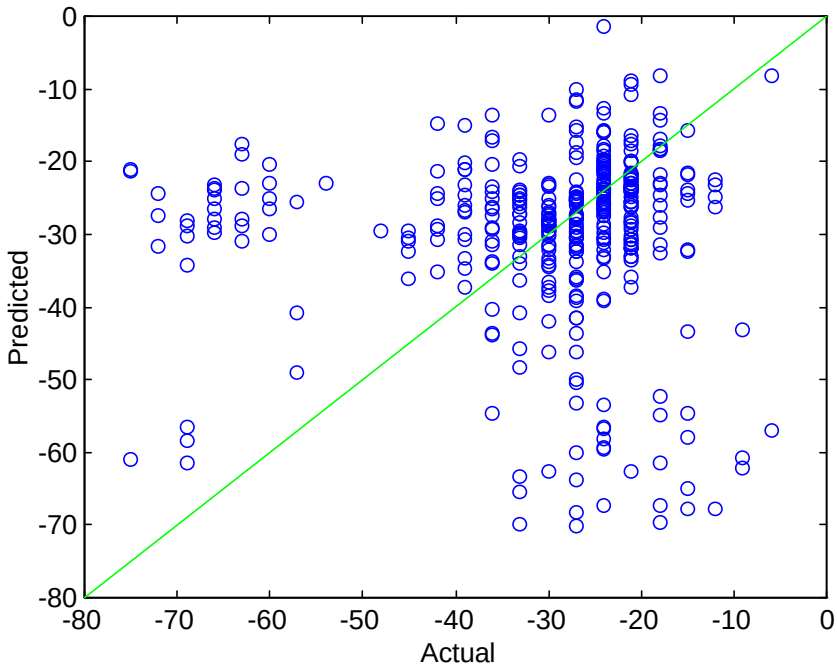

Figure 20. Validation for IBP.

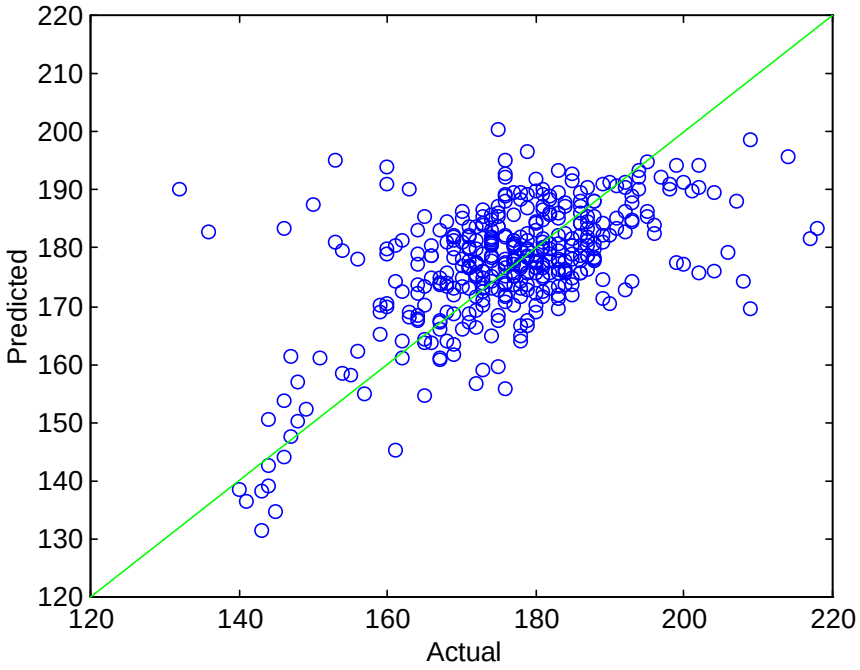

Figure 21. Validation for BP10.

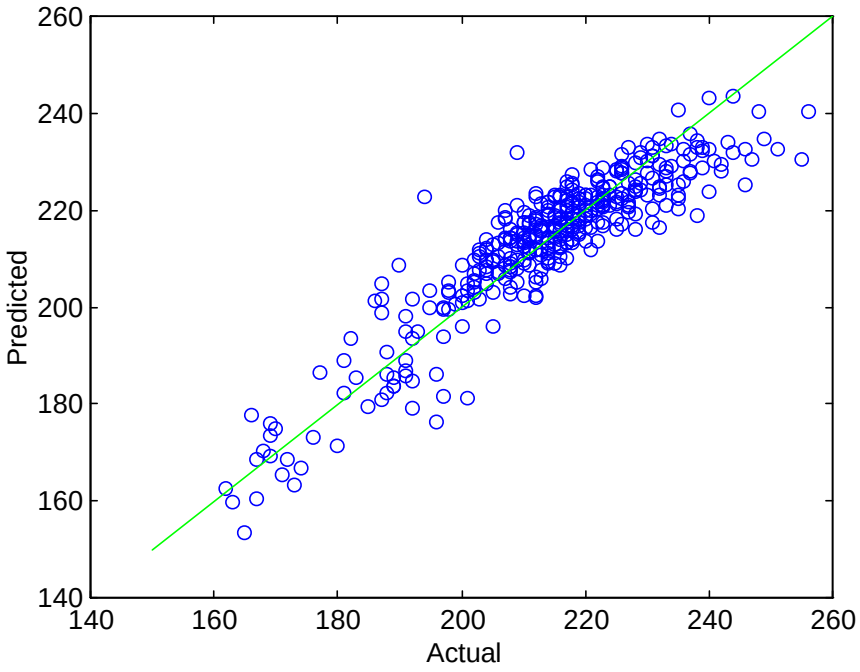

Figure 22. Instrument 2.
Validation for BP90.

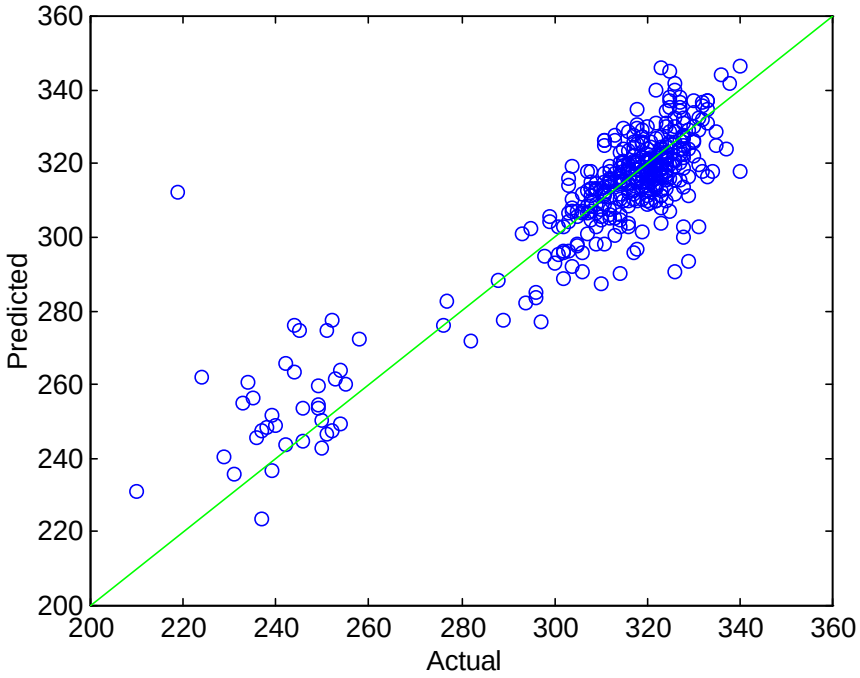

Figure 23. Instrument 2.
Validation for BP95.

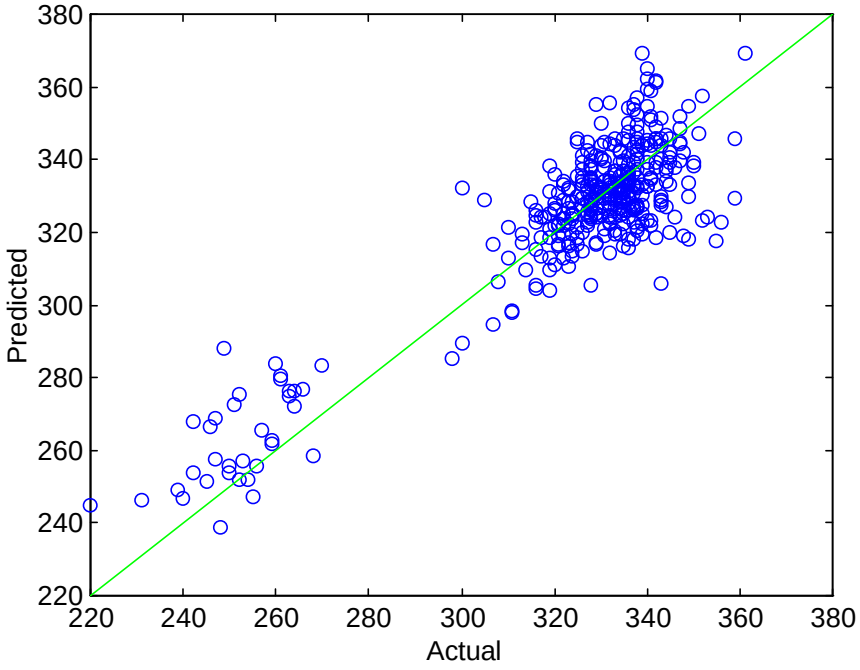

Figure 24. Instrument 2.
Validation for BPEP.

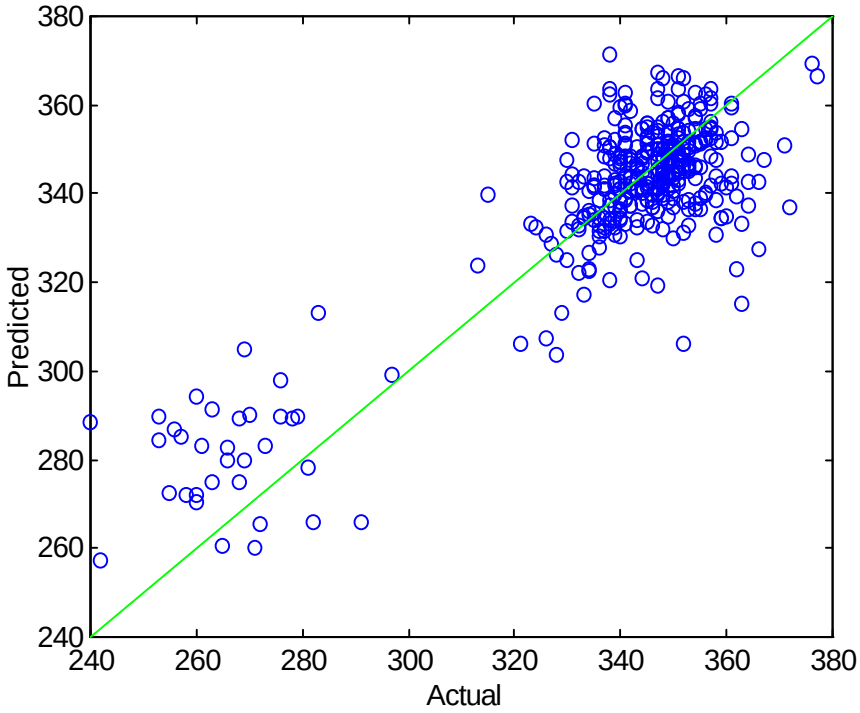

Figure 25. Instrument 2.
Validation for Cetane Index (D976).

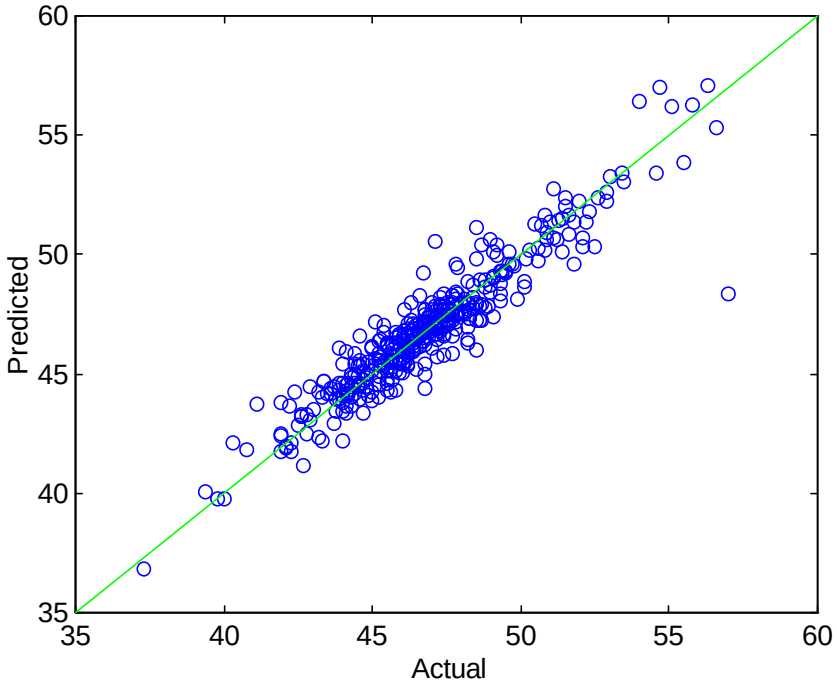

Figure 26. Instrument 2.
Validation for Hydrogen Content.

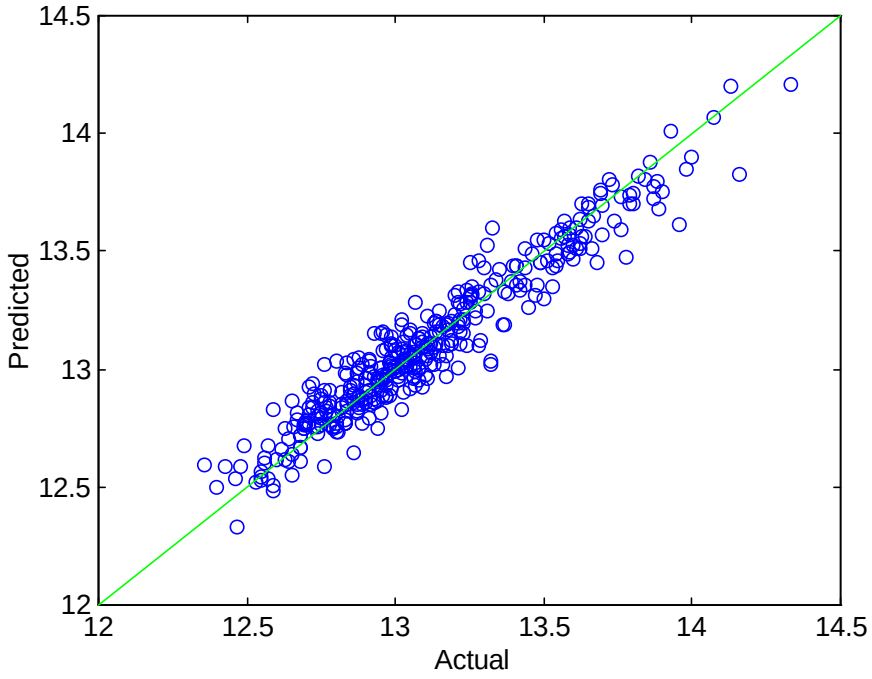

Figure 27. Instrument 2.
Validation for Carbon Content.

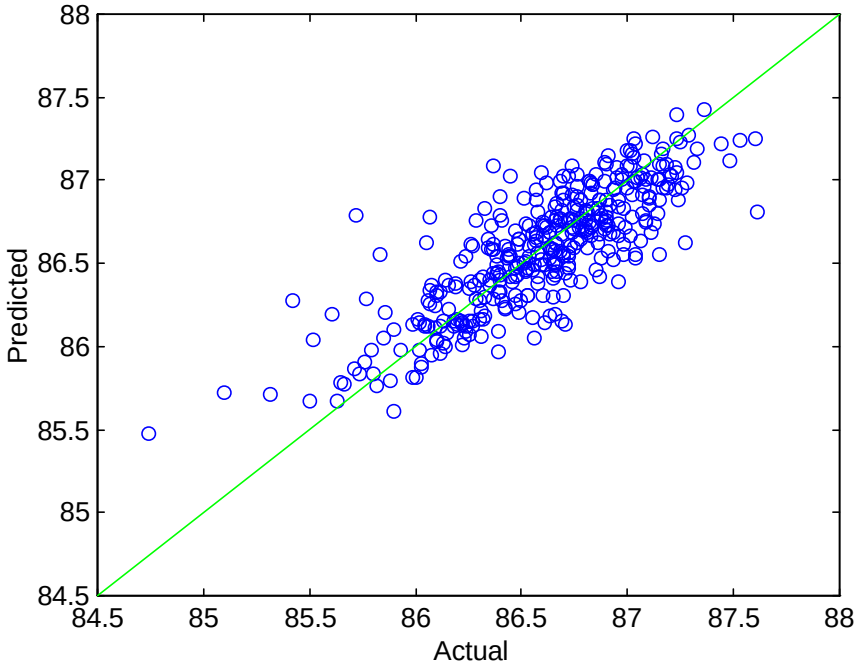

Figure 28. Instrument 2.
Validation for Carbon/Hydrogen.

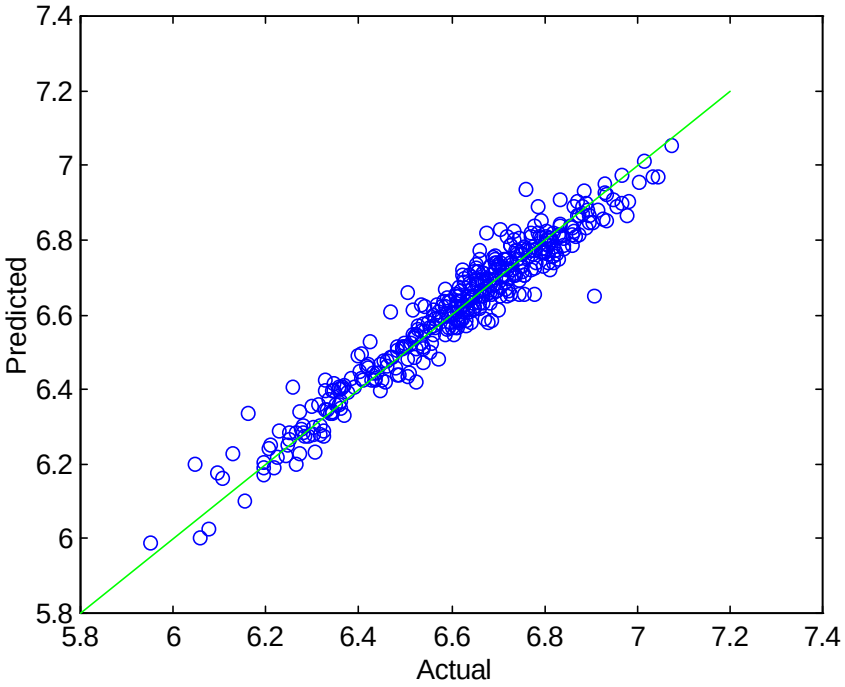

Figure 29. Instrument 2.
Validation for NHC (MJ/Kg).

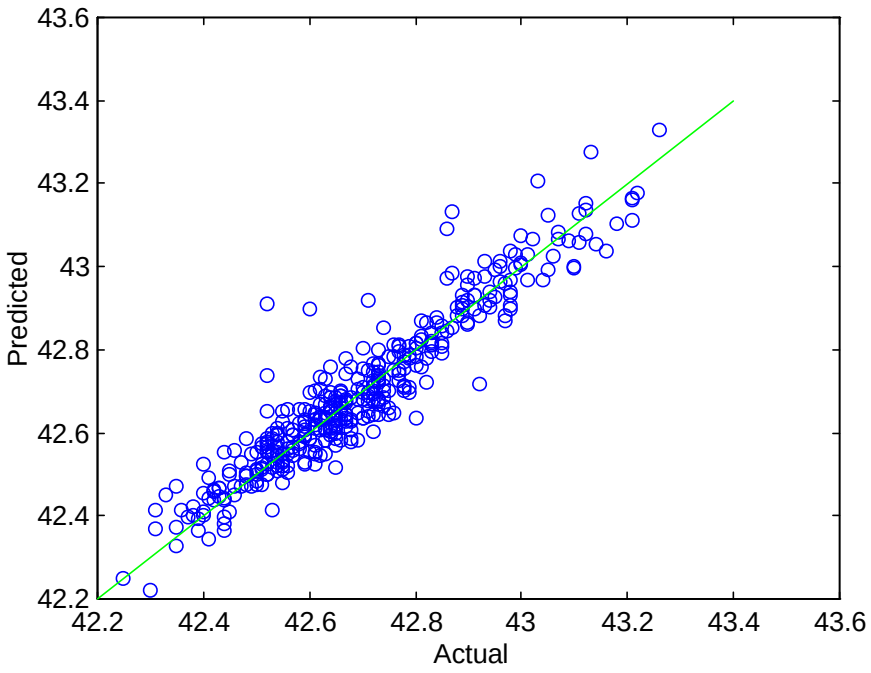

Figure 30. Instrument 2.
Validation for 1-ArH.

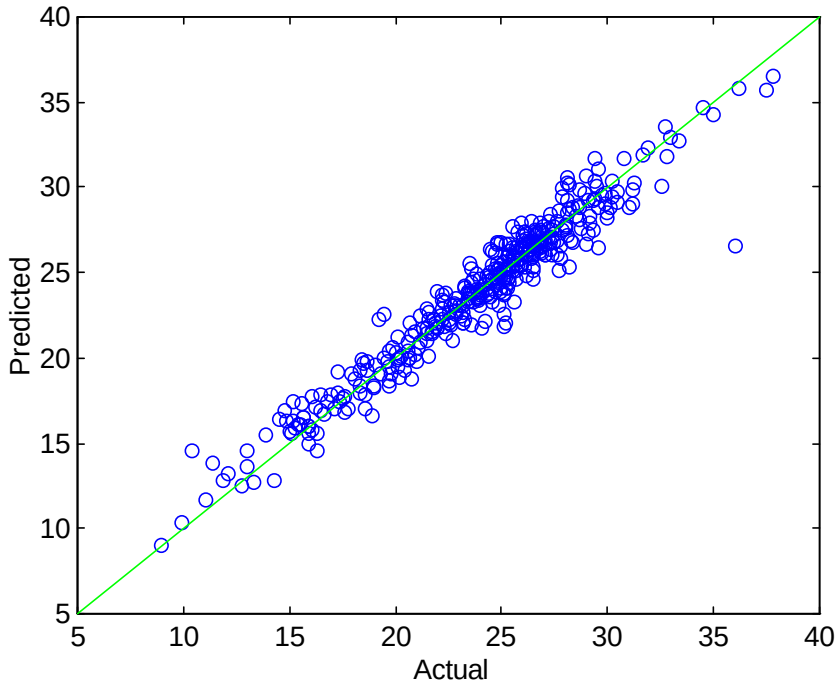

Figure 31. Instrument 2.
Validation for 2-ArH.

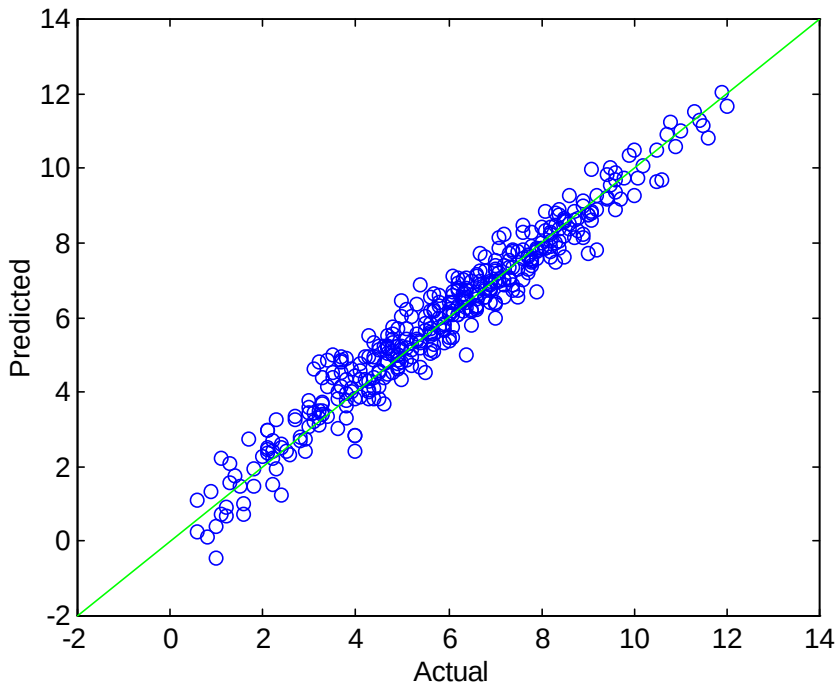

Figure 32. Instrument 2.
Validation for 3-ArH.